

Degenerate isostable reduction for fixed-point and limit-cycle attractors with defective linearizations

Dan Wilson

Department of Electrical Engineering and Computer Science, University of Tennessee, Knoxville, Tennessee 37996, USA

(Received 11 October 2020; accepted 2 February 2021; published 15 February 2021)

Isostable coordinates provide a convenient framework for understanding the transient behavior of dynamical systems with stable attractors. These isostable coordinates are often used to characterize the slowest decaying eigenfunctions of the Koopman operator; by neglecting the rapidly decaying Koopman eigenfunctions a reduced order model can be obtained. Existing work has focused primarily on nondegenerate isostable coordinates, that is, isostable coordinates that are associated with eigenvalues that have identical algebraic and geometric multiplicities. Current isostable reduction methods cannot be applied to characterize the decay associated with a defective eigenvalue. In this work, a degenerate isostable framework is proposed for use when eigenvalues are defective. These degenerate isostable coordinates are investigated in the context of various reduced order modeling frameworks that retain many of the important properties of standard (nondegenerate) isostable reduced modeling strategies. Reduced order modeling examples that require the use of degenerate isostable coordinates are presented with relevance to both circadian physiology and nonlinear fluid flows.

DOI: [10.1103/PhysRevE.103.022211](https://doi.org/10.1103/PhysRevE.103.022211)**I. INTRODUCTION**

Reduced order modeling techniques for high-dimensional, nonlinear dynamical systems have seen a surge of interest in recent years. Much of this interest has been focused on developing mathematical techniques based on Koopman analysis which can be used to understand the dynamics of a fully nonlinear system using a linear but infinite-dimensional operator [1–3]. To implement Koopman analysis for model reduction purposes, the identification of a suitable finite basis to represent the infinite-dimensional Koopman operator is a key necessity. Dynamic mode decomposition (DMD) is one strategy that has been developed to accomplish this task. DMD attempts to decompose the dynamical behavior of a nonlinear system into a set of linear modes with associated eigenvalues that govern their temporal evolution [4,5]. However, standard DMD algorithms generally return a large number of modes that are not sorted by order of importance making them difficult to apply in reduced modeling contexts. Strategies such as extended DMD have also been suggested which carefully select system observables; this strategy has been shown to be useful for some applications [6]. Other methods for identification of Koopman modes are actively being developed that incorporate deep learning approaches [7,8] and delay embedding of time-series data [9,10]. These strategies are particularly useful for systems for which the Koopman operator spectrum is continuous.

For nonlinear dynamical systems with stable attractors and a discrete Koopman operator spectrum, a powerful reduced coordinate framework is available that can be defined according to the slowest decaying modes of the Koopman operator. For such systems a so-called isostable coordinate framework encodes for the infinite time convergence to an attractor capturing level sets of the slowest decaying Koopman

eigenfunctions [11]. The notion of isostable coordinates was first investigated in [11] in the context of the infinite time behavior of solutions in the basin of attraction of a fixed point and later extended for use in periodic orbits [12–14]. Provided that some of the Koopman eigenfunctions decay rapidly, their contribution to the dynamics can be ignored resulting in an overall reduction in dimension. Furthermore, under the unperturbed flow of the underlying dynamical system, isostable coordinates exhibit exponential decay in the entire nonlinear basin of attraction. For this reason, they result in relatively simple reduced order models that can be investigated in a wide variety of control applications [14–19].

Various reduction strategies have been developed that leverage the isostable coordinate framework (for example, [11,14,17,20–22]) but they are all currently limited to use in systems where the eigenvalues associated with the linearized fixed point (or Floquet multipliers when the attractor is a periodic orbit) have equal algebraic and geometric multiplicities. In this work, a degenerate isostable coordinate framework is investigated for use when the linearizations of the underlying attractors have a defective eigenvalue (i.e., with unequal geometric and algebraic multiplicity). Ultimately, these degenerate isostable coordinates have similar properties to standard isostable coordinates; specifically, they have a relatively simple exponential decay in the entire basin of attraction that can be leveraged to identify reduced order models that accurately replicate nonlinear behaviors in the full order system. While defective matrices are rare from a statistical perspective, there are a number of applications where their use is required that are discussed in detail in the examples considered in this work.

The organization of this paper is as follows: Section II gives background information about nondegenerate isostable coordinates and discusses their utility for reduced order

modeling of limit-cycle and fixed-point attractors. Section III provides a definition for degenerate isostable coordinates that are valid when the eigenvalues of the linearized system (or Floquet multipliers of a periodic orbit) have unequal algebraic and geometric multiplicities. Section IV discusses the structure of and computation strategies for the terms of reduced order models that require the use of degenerate isostable coordinates. Section V gives two detailed reduced order modeling examples where standard isostable coordinates are not applicable and degenerate isostable coordinates must be used. Section VI gives concluding remarks.

II. BACKGROUND ON ISOSTABLE COORDINATE SYSTEMS FOR ANALYSIS OF TRANSIENT DYNAMICS

Consider an ordinary differential equation of the form

$$\dot{x} = F(x) + u(t), \tag{1}$$

where $x \in \mathbb{R}^N$ is the state, F gives the dynamics, and $u(t)$ is an external input. Here, background information about isostable coordinate transformations will be discussed for models of the form (1) that have stable attractors. Separate cases will be considered for fixed-point attractors and periodic-orbit attractors.

A. Isostable coordinates for fixed points

Isostable coordinates of fixed-point attractors can be computed by considering the infinite time behavior of (1) under the unperturbed flow which will be denoted by $\phi(t, x)$. Let x_0 be a stable fixed point of (1), and let $\Delta x = x - x_0$. Near this fixed point, the dynamics follow

$$\Delta \dot{x} = DF(x_0)\Delta x + O(|\Delta x|^2), \tag{2}$$

where $DF(x_0)$ is the Jacobian of F evaluated at the fixed point. Let $w_k, v_k,$ and λ_k be left eigenvectors, right eigenvectors, and eigenvalues of $DF(x_0)$, respectively. Additionally, let the eigenvalues be ordered according to $|\text{Re}(\lambda_k)| \leq |\text{Re}(\lambda_{k+1})|$ so that λ_1 represents the eigenvector with the slowest decay. Then, assuming the geometric multiplicity of λ_1 is identical to its algebraic multiplicity, as explained in [11], the principal isostable coordinate can be computed using Laplace averages

$$\psi_1(x) = \lim_{t \rightarrow \infty} \frac{1}{t} \int_0^t \{f \circ [\phi(s, x) - x_0]\} \exp(-\lambda_1 s) ds, \tag{3}$$

where $f \circ g$ denotes the composition of the function f with g and f is chosen so that $f \circ v_1 \neq 0$. In some cases, it is possible to give a constructive definition of isostable coordinates for some of the more slowly decaying components of the Koopman spectrum as

$$\psi_k(x) = \lim_{t \rightarrow \infty} \frac{1}{t} \int_0^t [w_k^T (\phi(s, x) - x_0)] \exp(-\lambda_k s) ds, \tag{4}$$

where T denotes the vector transpose. For $k = 1$, note that Eq. (4) can be written in the same form as (3). As discussed in detail in [23], the limit in (4) is not always guaranteed to exist for $k \geq 2$; in order for this limit to exist, $|\text{Re}(\lambda_k)|$ must be small enough relative to $|\text{Re}(\lambda_j)|$ for each $j < k$. This point is discussed in further detail in [23]. Note that taking the integral in Eqs. (3) and (4) is not absolutely necessary and an identical answer is obtained, for instance, if one takes

$\psi_k(x) = \lim_{t \rightarrow \infty} \{[w_k^T (\phi(t, x) - x_0)] \exp(-\lambda_k t)\}$ instead in (4). However, the formulation using Laplace averages can aid in numerical computation of the isostable coordinates.

For more rapidly decaying isostable coordinates, no constructive definition of the form (4) is possible. Instead, isostable coordinates can be defined implicitly as level sets of Koopman eigenfunctions with decay rates that depend on the eigenvalues of the linearization from Eq. (2). For the interested reader, [23] and [2] provide a detailed description of the expansion of dynamical systems in terms of Koopman eigenfunctions. A particularly useful feature of isostable coordinates is that they decay exponentially according to $\dot{\psi}_k = \lambda_k \psi_k$ when $u(t) = 0$ making them attractive as a reduced coordinate framework. Previous studies have investigated various problems that involve control of dynamical systems with fixed-point attractors using isostable reduced frameworks [11,24,25] (cf. [26]). Related control applications where solutions of partial differential equations are reduced using an isostable basis are considered in [27] and [28].

The above definitions for isostable coordinates (3) and (4) explicitly assume that the algebraic multiplicity of a given λ_k is identical to its geometric multiplicity. Very little about isostable coordinates has been studied for defective matrices for which the algebraic and geometric multiplicities of the eigenvalues are not equal. The authors of [11] suggest that an additional term can be added to the Laplace averages from (3), for instance, by replacing the $\exp(-\lambda_1 t)$ by $t^{1-m} \exp(-\lambda_1 t)$ for an eigenvalue with a size m Jordan block, but this strategy ignores $m - 1$ other modes that also decay at a rate proportional to $\exp(\lambda_1 t)$.

B. Isostable coordinates for periodic orbits

Isostable coordinates of periodic orbits can also be defined by invoking the notions of isochrons and asymptotic phase [29]. For the moment, it will be assumed that $u(t) = 0$ in order to analyze the unperturbed dynamics of (1). Supposing that (1) admits a T -periodic orbit $x^\gamma(t)$, one can define a phase $\theta \in [0, 2\pi)$ scaled so that $d\theta/dt = \omega$ on the limit cycle where $\omega = 2\pi/T$. The definition of phase can be extended to the basin of attraction of the limit cycle \mathcal{B}^γ using the notion of isochrons [29,30] to identify sets of initial conditions with the same infinite time behavior. More precisely, letting θ_1 be some phase corresponding to $a(0) \in x^\gamma$, the θ_1 isochron, Γ_{θ_1} , is defined as the set of all $b(0) \in \mathcal{B}^\gamma$ such that

$$\lim_{t \rightarrow \infty} \|a(t) - b(t)\| = 0, \tag{5}$$

where $\|\cdot\|$ can be any norm. The phase θ encodes for the asymptotic behavior of limit-cycle solutions and does not contain any information about the dynamics in directions transverse to the limit cycle, i.e., the amplitude coordinates. Many previous amplitude coordinate frameworks have been proposed [12,14,31–34], but this work will focus on the isostable coordinate framework. Previous work [13,19] has used Floquet theory [35] to define these coordinates in the fully nonlinear basin of attraction of the limit cycle and is summarized here. First, taking $\Delta x = x(\theta) - x^\gamma(\theta)$, to a linear approximation, one can write

$$\Delta \dot{x} = DF(\theta)\Delta x + O(|\Delta x|^2), \tag{6}$$

where DF denotes the Jacobian of the vector field evaluated at $x^\gamma(\theta)$. In the absence of input, θ simply increases at a rate governed by ω . Thus $DF(\theta)$ is T -periodic and (6) can be analyzed using Floquet theory. In this manner, let Φ be a fundamental matrix for which $x(T) = \Phi x(0)$ and let w_j, v_j, λ_j be left eigenvectors, right eigenvectors, and associated eigenvalues of Φ , respectively. Additionally, define $\kappa_j = \ln(\lambda_j)/T$ sorted so that $\kappa_N = 0$ (this is the Floquet exponent that is associated with the phase) with $|\operatorname{Re}(\kappa_j)| \leq |\operatorname{Re}(\kappa_{j+1})|$ for the remaining Floquet exponents so that κ_1 corresponds to the slowest decaying mode. For small magnitude κ_j with identical geometric and algebraic multiplicity, it is possible to define isostable coordinates explicitly according to

$$\psi_j(x) = \lim_{k \rightarrow \infty} [w_j^T (\phi(t_1^k, x) - x_0^\Gamma) \exp(-\kappa_j t_1^k)], \quad (7)$$

where t_1^k denotes the time of the k th transversal of the Γ_0 isochron, and x_0^Γ indicates the intersection of the periodic orbit with the Γ_0 isochron (i.e., $x \in \gamma$ with associated phase $\theta = 0$). Much like for isostable coordinates of fixed points, a constructive definition of the form (7) is generally unavailable for rapidly decaying isostable coordinates. Nevertheless, these faster decaying isostable coordinates can be defined implicitly as level sets of Koopman eigenfunctions with decay rates given by the Floquet exponents of the linearized system. More details of the Koopman spectrum and Koopman eigenfunctions are given in [23] and [2]. Similarly to the isostable coordinates for fixed points, in the entire basin of attraction of the periodic orbit, isostable coordinates decay according to $\dot{\psi}_j = \kappa_j \psi_j$ in the absence of input. This relationship can be exploited to define phase-amplitude reduced coordinate systems that are valid to arbitrary orders of accuracy in the phase and isostable coordinates [21].

Much like for isostable coordinates of fixed points, the definition (7) assumes that the eigenvalues associated with the slowest decaying eigenvectors of Φ have identical geometric and algebraic multiplicity. Comparatively very little has been studied about isostable coordinates associated with repeated eigenvalues with nonidentical geometric and algebraic multiplicities. The sections to follow provide a definition for these other exponentially decaying modes and investigate the resulting isostable coordinates in various reduced order modeling frameworks.

III. DEGENERATE ISOSTABLE COORDINATES FOR ATTRACTORS WITH A DEFECTIVE LINEARIZATION

In Eqs. (4) and (7), isostable coordinates are defined explicitly in terms of their exponential decay of solutions toward an attractor. In situations where the linearization (2) [resp., (6)] yields repeated eigenvalues (resp., Floquet multipliers) with Jordan blocks of size $m > 1$, these definitions are no longer possible because they do not match the infinite time decay. For the purposes of this work, isostable coordinates that are associated with a size $m > 1$ Jordan block will be referred to as degenerate isostable coordinates. Isostable coordinates that result from Jordan blocks of size $m = 1$ will be referred to as nondegenerate isostable coordinates. In this section, a definition for degenerate isostable coordinates is proposed that

gives m reduced coordinates for defective eigenvalues with size m Jordan blocks.

A. Degenerate isostable coordinates associated with a defective eigenvalue for fixed points

Let x_0 be a fixed point of (1). Suppose for a given linearization from (2) that λ_1 has an associated Jordan block of size m (recall that λ_1 is the smallest magnitude eigenvalue). Let $DF(x_0) = PJP^{-1}$ where J is the Jordan normal form, P is an invertible matrix, and $^{-1}$ denotes the matrix inverse. Also let $P_1 \in \mathbb{R}^{N \times m}$ and $W_1 \in \mathbb{R}^{N \times m}$ be defined so that $W_1^T DF(x_0) P_1 = J_1$ where J_1 is the Jordan block associated with λ_1 . With this definition, $W_1^T P_1 = \text{Id}$ where Id is an appropriately sized identity matrix. Intuitively, P_1 is composed of a basis of m generalized eigenvectors [36] associated with λ_1 , for example, where the generalized eigenvector of order k satisfies $[DF(x_0) - \lambda_1 \text{Id}]^k = 0$ and $[DF(x_0) - \lambda_1 \text{Id}]^{k-1} \neq 0$. A set of degenerate isostable coordinates can then be defined in a similar manner to (3) as

$$\Psi(x) = \lim_{t \rightarrow \infty} [\exp(-J_1 t) W_1^T (\phi(t, x) - x_0)], \quad (8)$$

where $\Psi = [\psi_1 \ \dots \ \psi_m]^T$ is a vector of the degenerate isostable coordinates. To aid in the explanation of the terms of (8), recall that λ_1 is the slowest decaying isostable coordinate so that in the limit as time approaches infinity,

$$\phi(t, x) - x_0 \approx P_1 \exp(J_1 t) S_0(x), \quad (9)$$

where $S_0(x)$ is a function that characterizes the infinite time behavior of the slowest decaying components of the solution. With this in mind, one finds that

$$\Psi(x) = S_0(x). \quad (10)$$

As suggested by [11], an alternative definition of degenerate isostables could instead be given by amending the definition (3) to replace $\exp(-\lambda_1 t)$ by $t^{1-m} \exp(-\lambda_1 t)$ to characterize slowest components of the infinite time decay toward the fixed point; in Sec. IV D this strategy is contrasted to the definition presented above. In general, when only the slowest components of the decay are considered for isostable coordinates associated with a size $m > 1$ Jordan block, the resulting coordinate system does not accurately reflect the dynamical behavior implemented in reduced order modeling strategies as observed in the example from Sec. V A.

B. Degenerate isostable coordinates associated with a defective eigenvalue for periodic orbits

Suppose that (1) admits a T -periodic orbit $x^\gamma(t)$ with isochrons defined according to (5). For a given fundamental matrix of (6), suppose that λ_1 (the nonunity eigenvalue with magnitude closest to 1) has an associated Jordan block of size m . Here, a similar strategy is implemented to define a set of m degenerate isostable coordinates associated with $\kappa_1 = \ln(\lambda_1)/T$. First, consider the matrix

$$\hat{\Phi} \equiv \ln(\Phi)/T = PJP^{-1}, \quad (11)$$

where J is the Jordan normal form and P is an invertible matrix. From this definition recalling Φ is the fundamental

matrix, one can verify that

$$\Phi = P \exp(JT)P^{-1}. \quad (12)$$

The above property will be used later. Additionally, define the matrices $P_1 \in \mathbb{R}^{N \times m}$ and $W_1 \in \mathbb{R}^{N \times m}$ so that $W_1^T \hat{\Phi} P_1 = J_1$, with $J_1 \in \mathbb{R}^{m \times m}$ being the Jordan block associated with κ_1 . As is the case when considering isostable coordinates of fixed points, $W_1^T P_1 = \text{Id}$ and P_1 is composed of a basis of m generalized eigenvectors of Φ associated with λ_1 . A set of associated isostable coordinates will be defined as

$$\Psi(x) = \lim_{k \rightarrow \infty} [\exp(-J_1 t_\Gamma^k) W_1^T (\phi(t_\Gamma^k, x) - x_0^\Gamma)], \quad (13)$$

where $\Psi = [\psi_1 \dots \psi_m]^T$ is a vector of degenerate isostable coordinates and t_Γ^k and x_0^Γ were defined below (7). This definition is similar to (8), except that the limit is taken in terms of the successive crossings of the Γ_0 isochron. To explain the individual terms of the definition (13), consider that in the limit as time approaches infinity, one can write

$$\phi(t_\Gamma^k, x) - x_0^\Gamma \approx P_1 \exp(J_1 t_\Gamma^k) S_0^\Gamma(x), \quad (14)$$

where $S_0^\Gamma(x)$ characterizes the infinite time behavior of the transformed coordinates with decay governed by the J_1 Jordan block. Thus, in the limit that k approaches infinity, one finds

$$\Psi(x) = S_0^\Gamma(x). \quad (15)$$

C. Unperturbed dynamics of degenerate isostable coordinates

As with the standard definition of isostable coordinates (4) and (7) for fixed points and periodic orbits, respectively, the definitions for degenerate isostable coordinates from (8) and (13) provide a coordinate framework with relatively simple unperturbed dynamics. To illustrate this point for systems with fixed points, consider any initial condition x in the basin of attraction of the fixed point. Comparing the isostable coordinates associated with the initial condition and the isostable coordinates Δt later as the system evolves under the flow, using the definition (8) one finds

$$\begin{aligned} \frac{d\Psi}{dt} &= \lim_{\Delta t \rightarrow 0} \frac{\Psi(\phi(\Delta t, x)) - \Psi(x)}{\Delta t} \\ &= \lim_{\Delta t \rightarrow 0} \frac{\exp(J_1 \Delta t) S_0(x) - S_0(x)}{\Delta t} \\ &= \lim_{\Delta t \rightarrow 0} \frac{[\exp(J_1 \Delta t) - \text{Id}] S_0(x)}{\Delta t} \\ &= J_1 S_0(x) \\ &= J_1 \Psi. \end{aligned} \quad (16)$$

Above, line 2 follows after substituting the limiting behavior from Eq. (9) into Eq. (8) and evaluating directly, line 4 can be obtained using the definition of the matrix exponential $\exp(X) = \sum_{k=0}^{\infty} \frac{1}{k!} X^k$, and line 5 follows directly from (10). Equation (16) illustrates a relatively simple decay of the degenerate isostable coordinates in the entire basin of attraction of the fixed point; as will be seen in the sections to follow, this structure makes the degenerate isostable coordinate framework useful as a reduced order modeling paradigm.

This decay is similar for isostable coordinates defined for periodic orbits. To see this, consider the definition (13) and let

$q^k(x) = \exp(-J_1 t_\Gamma^k) W_1^T (\phi(t_\Gamma^k, x) - x_0^\Gamma)$. Differentiating both sides of (13) with respect to time yields

$$\frac{d\Psi}{dt} = \lim_{k \rightarrow \infty} \left[\frac{\partial q^k}{\partial t_\Gamma^k} \frac{dt_\Gamma^k}{dt} \right]. \quad (17)$$

Recalling that $\phi(t_\Gamma^k, x)$ denotes the location of the k th crossing of the Γ_0 isochron, its partial derivative with respect to t_Γ^k is zero when no external perturbations are applied. Therefore, $\frac{\partial q^k}{\partial t_\Gamma^k} = -J_1 q^k$. Additionally, $\frac{dt_\Gamma^k}{dt} = -1$; i.e., the time at which the k th crossing of the Γ_0 section occurs decreases as the trajectory evolves under the flow. Substituting these relations into (17), one can write

$$\begin{aligned} \frac{d\Psi}{dt} &= \lim_{k \rightarrow \infty} [J_1 q^k] \\ &= J_1 \Psi. \end{aligned} \quad (18)$$

Similarly to the standard definition of nondegenerate isostable coordinates, the relationships (16) and (18) make the degenerate isostable coordinate framework particularly attractive for defining reduced order models as will be shown in the following sections.

IV. MODEL REDUCTION USING DEGENERATE ISOSTABLE COORDINATES

For the moment, consider a fixed-point attractor of (1) with degenerate isostable coordinates defined according to (8) corresponding to a size m Jordan block with eigenvalue λ_1 . Changing variables to isostable coordinates yields

$$\frac{d\psi_k}{dt} = \frac{\partial \psi_k}{\partial x} \cdot \frac{dx}{dt} = \frac{\partial \psi_k}{\partial x} \cdot [F(x) + u(t)], \quad (19)$$

where the dot denotes the dot product. For the moment letting $u(t) = 0$, from (16) recall that $d\Psi/dt = J_1 \Psi$. Thus, the individual isostable coordinate dynamics are $\dot{\psi}_k = \frac{\partial \psi_k}{\partial x} \cdot F(x) = \lambda_1 \psi_k + \mathcal{I}_k$ for $k < m$. When $u(t) \neq 0$, Eq. (19) can be written as

$$\begin{aligned} \dot{\psi}_k &= \lambda_1 \psi_k + \psi_{k+1} + \mathcal{I}_k(x) \cdot u(t), \\ k &= 1, \dots, m-1, \end{aligned} \quad (20)$$

where $\mathcal{I}_k(x) \equiv \frac{\partial \psi_k}{\partial x}$ with partial derivatives are evaluated at x . Using similar reasoning, the remaining isostable coordinate evolves according to

$$\dot{\psi}_m = \lambda_1 \psi_m + \mathcal{I}_m(x) \cdot u(t). \quad (21)$$

If the underlying attractor is a periodic orbit, rather than a fixed point, the equations describing the isostable dynamics (20) and (21) are the same, except that the λ_1 values are replaced by κ_1 values. Note that for a periodic orbit, the gradients \mathcal{I}_k will also be functions of the phase.

In order to identify a closed set of equations to describe the degenerate isostable reduced coordinates in response to inputs, it is necessary to compute $\mathcal{I}_k(x)$ in terms of the isostable coordinates themselves rather than x . The following sections present a strategy for computing the necessary terms of such reduced order models when using degenerate isostable coordinates.

A. Phase and degenerate isostable reduced equations for periodic orbits

Here, a reduction is considered that describes the dynamical behavior near a periodic orbit with a defective fundamental matrix

$$\begin{aligned}\dot{\theta} &= \omega + \mathcal{Z}(\theta, \psi_1, \dots, \psi_m) \cdot u(t), \\ \dot{\psi}_k &= \kappa_1 \psi_k + \psi_{k+1} + \mathcal{I}_k(\theta, \psi_1, \dots, \psi_m) \cdot u(t), \\ k &= 1, \dots, m-1, \\ \dot{\psi}_m &= \kappa_1 \psi_m + \mathcal{I}_m(\theta, \psi_1, \dots, \psi_m) \cdot u(t), \\ x &= x^\gamma(\theta) + \mathcal{G}(\theta, \psi_1, \dots, \psi_m).\end{aligned}\quad (22)$$

Above, it is assumed that ψ_1, \dots, ψ_m are degenerate isostable coordinates that result from a size m Jordan block. As part of the reduction (22), it is assumed that all other Floquet exponents κ_j with $j > m$ are large in magnitude so that they die out rapidly and can be ignored from the reduction. The terms \mathcal{Z} , \mathcal{I}_k , and \mathcal{G} (the phase response, isostable response, and deviation from the periodic orbit, respectively) will be found through asymptotic expansion in terms of the degenerate isostable coordinates. A similar reduced order model was considered in [21] and is valid for nondegenerate isostable coordinates. Necessary modifications to the strategies presented in [21] will be discussed below in order to accommodate degenerate isostable coordinates.

1. Asymptotic expansion of the state in terms of degenerate isostable coordinates

When computing asymptotic expansions of the terms of (22), it is necessary to start with \mathcal{G} :

$$\mathcal{G}(\theta, \psi_1, \dots, \psi_m) = \sum_{k=1}^m [\psi_k g^k(\theta)] + \sum_{j=1}^m \sum_{k=1}^j [\psi_j \psi_k g^{jk}(\theta)] + \sum_{i=1}^m \sum_{j=1}^i \sum_{k=1}^j [\psi_i \psi_j \psi_k g^{ijk}(\theta)] + \dots \approx \Delta x. \quad (23)$$

Above, each $g^{ijk\dots}(\theta)$ can be thought of as a nonlinear analog to a Floquet eigenfunction of the linearized system. The approximate equality comes from the fact that the more rapidly decaying isostable coordinates are assumed to be zero so that (23) gives the behavior on a hypersurface determined by the nonzero isostable coordinates. Taking the input $u(t) = 0$ so that the decay follows $\frac{d}{dt}\Psi = J_1\Psi$ as in Eq (18), the relationships of the form (20) and (21) can be exploited when taking the time derivative of (23):

$$\frac{d\Delta x}{dt} = \sum_{k=1}^m \left[\frac{dg^k}{dt} \psi_k + g^k(\psi_k \kappa_1 + \psi_{k+1}) \right] + \sum_{j=1}^m \sum_{k=1}^j \left[\frac{dg^{jk}}{dt} \psi_j \psi_k + 2g^{jk} \psi_j \psi_k \kappa_1 + g^{jk}(\psi_j \psi_{k+1} + \psi_k \psi_{j+1}) \right] + \dots \quad (24)$$

Note that in the above equation, there are only m nonzero isostable coordinates considered and that $\psi_{m+1} \equiv 0$ is used as a placeholder to write the summations with more compact notation; additionally, the explicit θ dependence for each function of the form $g^{ijk\dots}$ has been suppressed for convenience of notation. One can also write $d\Delta x/dt$ directly using the Taylor expansion of (1) with $u(t) = 0$. Using the result (A3) from Appendix A and substituting (23) in for Δx yields

$$\frac{d\Delta x}{dt} = DF(x(\theta)) \left[\sum_{k=1}^m [\psi_k g^k(\theta)] + \sum_{j=1}^m \sum_{k=1}^j [\psi_j \psi_k g^{jk}(\theta)] + \dots \right] + Q(\Delta x), \quad (25)$$

where

$$Q(\Delta x) = \begin{bmatrix} \sum_{i=2}^{\infty} \frac{1}{i!} \left[\otimes \left[\sum_{k=1}^m [\psi_k g^k(\theta)] + \sum_{j=1}^m \sum_{k=1}^j [\psi_j \psi_k g^{jk}(\theta)] + \dots \right]^T \right] \text{vec}(f_1^{(i)}(\theta)) \\ \vdots \\ \sum_{i=2}^{\infty} \frac{1}{i!} \left[\otimes \left[\sum_{k=1}^m [\psi_k g^k(\theta)] + \sum_{j=1}^m \sum_{k=1}^j [\psi_j \psi_k g^{jk}(\theta)] + \dots \right]^T \right] \text{vec}(f_N^{(i)}(\theta)) \end{bmatrix}, \quad (26)$$

with each partial derivative of the form $f_j^{(k)}(\theta)$ evaluated at $x(\theta)$ on the limit cycle. Noticing that (25) and (24) are identical, both sides can be equated and relationships between the functions of the expansion can be found by matching powers of the isostable coefficients in each equation. An explicit example of this process and subsequent strategies for computation of the terms of (23) is given in Sec. IV A 4 to follow.

2. Asymptotic expansion of the gradient of the phase in terms of degenerate isostable coordinates

As illustrated in [21] (cf. [37]) along trajectories, under the unperturbed flow, the gradient of the phase coordinate evolves according to

$$\frac{d\mathcal{Z}}{dt} = - \left. \frac{\partial F^T}{\partial x} \right|_x \mathcal{Z}. \quad (27)$$

Much like \mathcal{G} , the gradient of the phase can be written as an asymptotic expansion in the degenerate isostable coordinates centered at the periodic orbit,

$$\mathcal{Z}(\theta, \psi_1, \dots, \psi_m) = Z(\theta) + \sum_{k=1}^m [\psi_k Z^k(\theta)] + \sum_{j=1}^m \sum_{k=1}^j [\psi_j \psi_k Z^{jk}(\theta)] + \sum_{i=1}^m \sum_{j=1}^i \sum_{k=1}^j [\psi_i \psi_j \psi_k Z^{ijk}(\theta)] + \dots, \quad (28)$$

where $Z(\theta)$ is the gradient of the phase evaluated on the periodic orbit and terms of the form $Z^{ijk\dots}$ represent higher order corrections. Taking the time derivative of (28) yields

$$\begin{aligned} \frac{d\mathcal{Z}}{dt} &= \frac{dZ}{dt} + \sum_{k=1}^m \left[\frac{dZ^k}{dt} + Z^k(\psi_k \kappa_1 + \psi_{k+1}) \right] \\ &+ \sum_{j=1}^m \sum_{k=1}^j \left[\frac{dZ^{jk}}{dt} \psi_k \psi_j + 2Z^{jk} \psi_j \psi_k \kappa_1 + Z^{jk}(\psi_j \psi_{k+1} + \psi_k \psi_{j+1}) \right] + \dots, \end{aligned} \quad (29)$$

where, once again, relationships of the form (20) and (21) are substituted for the time derivatives of the isostable coordinates and $\psi_{m+1} \equiv 0$ is used as a placeholder for notational convenience. Substituting (29) into the left hand side of (27) and both (28) and (B1) into the right hand side of (27) yields

$$\frac{d\mathcal{Z}}{dt} + \sum_{k=1}^m \left[\frac{dZ^k}{dt} + Z^k(\psi_k \kappa_1 + \psi_{k+1}) \right] + \dots = -DF^T(x(\theta)) \left(Z(\theta) + \sum_{k=1}^M [\psi_k Z^k(\theta)] + \dots \right) - Q_\theta(\Delta x, \mathcal{Z}), \quad (30)$$

where

$$Q_\theta(\Delta x, \mathcal{Z}) = [a_1 \quad \dots \quad a_N] \left(Z(\theta) + \sum_{k=1}^m [\psi_k Z^k(\theta)] + \dots \right). \quad (31)$$

In (30) and (31), all functions are evaluated at $x(\theta)$ on the limit cycle. Relationships for the terms of the asymptotic expansion can be obtained by matching powers of the isostable coefficients in Eq. (30). An example of this process and subsequent strategies for computation of the terms of (28) is given in Sec. IV A 4.

3. Asymptotic expansion of the gradient of the degenerate isostable coordinates

In order to derive equations associated with the gradient of the degenerate isostable coordinates, consider any unperturbed trajectory of (1) in the basin of attraction of the periodic orbit $x(t)$. Additionally, consider any perturbed trajectory x_1 that has been shifted by an infinitesimal amount Δx with $\|x - x_1\| = O(\epsilon)$ where $0 < \epsilon \ll 1$. The shift in a given ψ_n caused by this initial perturbation is

$$\Delta \psi_n = \Delta x^T \mathcal{I}_n(\theta, \psi_1, \dots, \psi_M). \quad (32)$$

First, consider the case for which $n \leq m - 1$. Noting that $\frac{d}{dt} \Delta \psi_n = \kappa_1 \Delta \psi_n + \Delta \psi_{n+1}$, taking the time derivative of both sides of (32) yields

$$\kappa_1 \Delta \psi_n + \Delta \psi_{n+1} = \frac{d\Delta x^T}{dt} \mathcal{I}_n + \Delta x^T \frac{d\mathcal{I}_n}{dt}. \quad (33)$$

Rearranging (33) yields

$$\begin{aligned} 0 &= -\kappa_1 \Delta x^T \mathcal{I}_n - \Delta x^T \mathcal{I}_{n+1} + \frac{d\Delta x^T}{dt} \mathcal{I}_n + \Delta x^T \frac{d\mathcal{I}_n}{dt} \\ &= \Delta x^T \left[\left(\frac{\partial F^T}{\partial x} \Big|_x - \kappa_1 \text{Id} \right) \mathcal{I}_n + \frac{d\mathcal{I}_n}{dt} - \mathcal{I}_{n+1} \right], \end{aligned} \quad (34)$$

where in the second line $d\Delta x^T/dt$ is approximated by $\Delta x^T (\partial F^T / \partial x)|_x$. Noting that Δx is arbitrary, the terms inside the brackets of (34) must be zero so that

$$\begin{aligned} \frac{d\mathcal{I}_n}{dt} &= - \left(\frac{\partial F^T}{\partial x} \Big|_x - \kappa_1 \text{Id} \right) \mathcal{I}_n + \mathcal{I}_{n+1}, \\ n &= 1, \dots, m - 1. \end{aligned} \quad (35)$$

A similar argument can be followed to find

$$\frac{d\mathcal{I}_m}{dt} = - \left(\frac{\partial F^T}{\partial x} \Big|_x - \kappa_1 \text{Id} \right) \mathcal{I}_m. \quad (36)$$

Equations (35) and (36) can be used to expand the isostable response curves in powers of the degenerate isostable coordinates. Similarly to the computation strategy for the terms of the phase response curves, the gradient of the isostable coordinates can be written as

$$\mathcal{I}_n(\theta, \psi_1, \dots, \psi_m) = I_n(\theta) + \sum_{k=1}^m [\psi_k I_n^k(\theta)] + \sum_{j=1}^m \sum_{k=1}^j [\psi_j \psi_k I_n^{jk}(\theta)] + \sum_{i=1}^m \sum_{j=1}^i \sum_{k=1}^j [\psi_i \psi_j \psi_k I_n^{ijk}(\theta)] + \dots, \quad (37)$$

where $I_n(\theta)$ is the gradient of the isostable response curve evaluated on the periodic orbit at phase θ and $I_n^{ijk\dots}$ give higher order corrections. The time derivative of (37) is

$$\frac{d\mathcal{I}_n}{dt} = \frac{dZ}{dt} + \sum_{k=1}^m \left[\frac{dI_n^k}{dt} + Z^k(\psi_k \kappa_1 + \psi_{k+1}) \right] + \sum_{j=1}^m \sum_{k=1}^j \left[\frac{dI_n^{jk}}{dt} \psi_j \psi_k + 2I_n^{jk} \psi_j \psi_k \kappa_1 + I_n^{jk}(\psi_j \psi_{k+1} + \psi_k \psi_{j+1}) \right] + \dots, \quad (38)$$

where the time derivatives of each isostable coordinate of the form (20) and (21) are used to derive the above expression. Once again, $\psi_{m+1} \equiv 0$ is used above as a placeholder for notational convenience. Similarly to the previous section, substituting (38) into the left hand sides of both (35) and (36), and simultaneously substituting (37) and (B1) into the right hand side of (35) and (36), gives

$$\begin{aligned} \frac{dI_n}{dt} + \sum_{k=1}^m \left[\frac{dI_n^k}{dt} + I_n^k(\psi_k \kappa_1 + \psi_{k+1}) \right] + \dots = -[DF^T(x(\theta)) - \kappa_1 \text{Id}] \left(I_n(\theta) + \sum_{k=1}^m [\psi_k I_n^k(\theta)] + \dots \right) - Q_{\psi_n}(\Delta x, \mathcal{I}_n) \\ + \left(I_{n+1}(\theta) + \sum_{k=1}^m [\psi_k I_{n+1}^k(\theta)] + \sum_{j=1}^m \sum_{k=1}^j [\psi_j \psi_k I_{n+1}^{jk}(\theta)] + \dots \right), \end{aligned} \quad (39)$$

where

$$Q_{\psi_n}(\Delta x, \mathcal{I}_n) = [a_1 \quad \dots \quad a_N] \left(I_n(\theta) + \sum_{k=1}^m [\psi_k I_n^k(\theta)] + \sum_{j=1}^m \sum_{k=1}^j [\psi_j \psi_k I_n^{jk}(\theta)] + \dots \right), \quad (40)$$

for $n = 1, \dots, m$. Note that while there are only m isostable coordinates, and hence m isostable response curves, $\mathcal{I}_{m+1} \equiv 0$ is used as a placeholder for notational convenience so that $I_{m+1}(\theta), I_{m+1}^1(\theta), I_{m+1}^2(\theta), \dots$ are all equal to zero. In (39) and (40), all functions are evaluated at $x(\theta)$ on the limit cycle. Much like for the terms of the gradient of the phase coordinates, relationships for the terms of the asymptotic expansion of the isostable coordinates can be obtained by matching powers of the isostable coefficients in Eq. (39). Specific examples for computing the necessary terms of \mathcal{G}, \mathcal{Z} , and each \mathcal{I}_n are given in the next section.

4. Example and strategies for computing the terms of the reduction for Jordan blocks of size two

The previous sections provide relationships that can be used to identify the expansions \mathcal{G} [using (24) and (25)], \mathcal{Z} [using (30)], and \mathcal{I}_n [using (39)] for the phase and degenerate isostable reduced equations of (1). Here, a detailed strategy for computing these terms is given that is valid for systems with two degenerate isostable coordinates. Note that reduced equations for degenerate isostable coordinates with Jordan blocks of size larger than 2 can also be considered using an approach similar to the one presented here.

It will be assumed that a T -periodic orbit $x^\nu(t)$ has already been identified and that the fundamental matrix Φ has a size 2 Jordan block with associated Floquet exponent κ_1 . It will also be assumed that the remaining Floquet exponents are large in magnitude so that the degenerate isostable coordinates are the only amplitude coordinates considered.

Step 1: Computing the terms of \mathcal{G} . As stated in the previous section, relationships for each term in the expansion of \mathcal{G} from (23) can be found by matching the appropriate powers of the isostable coordinates after equating (24) and (25). Using a symbolic computational package, one can group the terms of $Q(\Delta x)$ according to

$$Q(\Delta x) = \sum_{j=1}^m \sum_{k=1}^j [\psi_j \psi_k Q^{jk}] + \sum_{i=1}^m \sum_{j=1}^i \sum_{k=1}^j [\psi_i \psi_j \psi_k Q^{ijk}] + \dots \quad (41)$$

Matching powers to leading order ψ_1 and ψ_2 respectively yields relationships for the first order terms of the expansion of \mathcal{G}

$$\dot{g}^1 = (DF - \kappa_1 \text{Id})g^1, \quad (42)$$

$$\dot{g}^2 = (DF - \kappa_1 \text{Id})g^2 - g^1, \quad (43)$$

where all partial derivatives and functions are evaluated at $x(\theta)$ on the limit cycle. The terms g^1 and g^2 are the periodic solutions to (42) and (43), respectively. Note that because $\dot{g}^1 = DF g^1$ has a Floquet exponent of κ_1 then $\dot{g}^1 = (DF - \kappa_1 \text{Id})g^1$ has a zero

Floquet exponent and must be appropriately normalized. The periodic solution to (43) also requires normalization for the same reason. Here, this normalization will be accomplished by letting $g^1(\theta) = P_1[1 \ 0]^T$ and $g^2(\theta) = P_1[0 \ 1]^T$ for $\theta = 0$ where P_1 was defined just before Eq. (13). For the second order accurate terms, one finds

$$\begin{aligned}\dot{g}^{11} &= (DF - 2\kappa_1 \text{Id})g^{11} + Q^{11}, \\ \dot{g}^{12} &= (DF - 2\kappa_1 \text{Id})g^{12} + Q^{12} - 2g^{11}, \\ \dot{g}^{22} &= (DF - 2\kappa_1 \text{Id})g^{22} + Q^{22} - g^{12}.\end{aligned}\quad (44)$$

When considering higher order terms, a general pattern emerges:

$$\begin{aligned}\dot{g}^{\alpha\beta}_{12} &= [DF - (\alpha + \beta)\kappa_1 \text{Id}]g^{\alpha\beta}_{12} + Q^{\alpha\beta}_{12}, \quad \text{for } \beta = 0, \\ \dot{g}^{\alpha\beta}_{12} &= [DF - (\alpha + \beta)\kappa_1 \text{Id}]g^{\alpha\beta}_{12} + Q^{\alpha\beta}_{12} - (\alpha + 1)g^{\frac{\alpha+1}{1} \frac{\beta-1}{2}}, \quad \text{for } \beta > 0,\end{aligned}\quad (45)$$

where, for instance, the notation $g^{\frac{32}{12}}$ represents the term g^{11122} . Each $g^{\alpha\beta}_{12}$ can be computed by finding a periodic solution to an equation of the form (45). Additionally, each term of $Q^{\alpha\beta}_{12}$ can only contain lower order terms of the expansion; for instance, Q^{11} may depend on second and first order terms such as g^{11} or g^2 but will not contain terms of the form g^{122} (i.e., third order and higher). Thus, all of the terms of \mathcal{G} can be computed in the following order g^1, g^2 (first order terms), g^{11}, g^{12}, g^{22} (second order terms), $g^{111}, g^{112}, g^{122}, g^{222}$ (third order terms), and so on.

Step 2: Computing the terms of \mathcal{Z} . Computation of the phase response curve is similar to computation of the expansion of \mathcal{G} from the previous step. This can be accomplished by matching the appropriate terms of the isostable coordinates in Eq. (30). Once again, a symbolic computational package can be used to group the terms of $Q_\theta(\Delta x, \mathcal{Z})$ according to

$$Q_\theta(\Delta x, \mathcal{Z}) = \sum_{k=1}^m [\psi_k Q_\theta^k] + \sum_{j=1}^m \sum_{k=1}^j [\psi_j \psi_k Q_\theta^{jk}] + \sum_{i=1}^m \sum_{j=1}^i \sum_{k=1}^j [\psi_i \psi_j \psi_k Q_\theta^{ijk}] + \dots \quad (46)$$

As was the case with $Q(\Delta x)$, each term of the form $Q_\theta^{ijk}(\Delta x, \mathcal{Z})$ only depends on lower order terms of the expansion of \mathcal{Z} and \mathcal{G} . For instance, Q_θ^{111} may depend on terms Z^{11} or Z^2 but will not contain terms of the form Z^{122} . Matching the zeroth order terms of (30) yields the familiar adjoint equation

$$\dot{Z}(\theta) = -DFZ, \quad (47)$$

with a periodic solution that must be normalized according to $\omega = F(x)^T Z$. The remaining terms follow a similar pattern to the one described in (45),

$$\begin{aligned}\dot{Z}^{\alpha\beta}_{12} &= -[DF + (\alpha + \beta)\kappa_1 \text{Id}]Z^{\alpha\beta}_{12} - Q_\theta^{\alpha\beta}_{12}, \quad \text{for } \beta = 0, \\ \dot{Z}^{\alpha\beta}_{12} &= -[DF + (\alpha + \beta)\kappa_1 \text{Id}]Z^{\alpha\beta}_{12} - Q_\theta^{\alpha\beta}_{12} - (\alpha + 1)Z^{\frac{\alpha+1}{1} \frac{\beta-1}{2}}, \quad \text{for } \beta > 0,\end{aligned}\quad (48)$$

where the solution to each term of the expansion represents a periodic solution to an equation of the form (48). Because (48) has a similar structure to (45), the terms of the phase response curves can be calculated in the same progression, i.e., by finding Z (zeroth order), followed by Z^1 then Z^2 (first order), followed by Z^{11} then Z^{12} then Z^{22} (second order), and so on. To ensure numerical stability, it is usually necessary to solve the equations of the form (48) backward in time.

Step 3: Computing the terms of each \mathcal{I}_n . The equations required to compute the terms of each \mathcal{I}_n can be found by matching appropriate terms of the isostable coordinates in equations of the form (39). As with the other terms of the reduction, a symbolic computational package can be used to group the terms of $Q_{\psi_n}(\Delta x, \mathcal{I}_n)$ as

$$Q_{\psi_n}(\Delta x, \mathcal{I}_n) = \sum_{k=1}^m [\psi_k Q_{\psi_n}^k] + \sum_{j=1}^m \sum_{k=1}^j [\psi_j \psi_k Q_{\psi_n}^{jk}] + \sum_{i=1}^m \sum_{j=1}^i \sum_{k=1}^j [\psi_i \psi_j \psi_k Q_{\psi_n}^{ijk}] + \dots \quad (49)$$

Much like in (46), p th order terms of Q_{ψ_n} in the isostable coordinates only depend on terms up to $(p - 1)$ th order in the Δx and \mathcal{I}_n expansion. When two degenerate isostable coordinates are considered, the zeroth order terms of the expansion are found to be

$$\dot{I}_1 = -(DF - \kappa_1 \text{Id})I_1 + I_2, \quad (50)$$

$$\dot{I}_2 = -(DF - \kappa_1 \text{Id})I_2, \quad (51)$$

where I_1 and I_2 are periodic solutions to (50) and (51). Notice that because the equation for I_1 requires knowledge of I_2 , one must first solve (51) before solving (50). The solutions of these equations must be normalized by $I_1^T g^1 = 1$ and $I_2^T g^2 = 1$. The higher order terms associated with \mathcal{I}_1 can be computed according to

$$\begin{aligned} \dot{I}_1^{\alpha\beta} &= -[DF + (\alpha + \beta - 1)\kappa_1 \text{Id}]I_1^{\alpha\beta} - Q_{\psi_1}^{\alpha\beta} + I_2^{\alpha\beta}, \quad \text{for } \beta = 0, \\ \dot{I}_1^{\alpha\beta} &= -[DF + (\alpha + \beta - 1)\kappa_1 \text{Id}]I_1^{\alpha\beta} - Q_{\psi_1}^{\alpha\beta} + I_2^{\alpha\beta} - (\alpha + 1)I_1^{\frac{\alpha+1}{2} \frac{\beta-1}{2}}, \quad \text{for } \beta > 0. \end{aligned} \quad (52)$$

The higher order terms associated with \mathcal{I}_2 can be found according to

$$\begin{aligned} \dot{I}_2^{\alpha\beta} &= -[DF + (\alpha + \beta - 1)\kappa_1 \text{Id}]I_2^{\alpha\beta} - Q_{\psi_2}^{\alpha\beta}, \quad \text{for } \beta = 0, \\ \dot{I}_2^{\alpha\beta} &= -[DF + (\alpha + \beta - 1)\kappa_1 \text{Id}]I_2^{\alpha\beta} - Q_{\psi_2}^{\alpha\beta} - (\alpha + 1)I_2^{\frac{\alpha+1}{2} \frac{\beta-1}{2}}, \quad \text{for } \beta > 0. \end{aligned} \quad (53)$$

Similarly to both \mathcal{Z} and \mathcal{G} , each of the terms of the expansion of the isostable response curves can be computed by finding periodic solutions of (52) and (53). Noticing that the terms of (52) depend on the terms of (53) the expansion of \mathcal{I}_2 must be computed before the terms of \mathcal{I}_1 . Additionally, because (52) and (53) have similar structures to (45), the terms for a given \mathcal{I}_n must be calculated in the following progression: I_n (zeroth order), followed by I_n^1 then I_n^2 (first order), followed by I_n^{11} then I_n^{12} then I_n^{22} (third order), and so on. To ensure numerical stability it is generally necessary to solve equations of the form (52) and (53) backward in time.

As a final note, normalization will be necessary for terms of the expansion of the isostable response curves of the form I_j^k with $j, k \in \{1, 2\}$. To see this, simplifying either (52) or (53) when $j, k \in \{1, 2\}$ yields equations of the form

$$\dot{I}_j^k = -DF I_j^k + p_j^k, \quad (54)$$

where p_j^k represent periodic terms that do not depend on I_j^k . The homogeneous solution has a nonzero kernel; intuitively each p_j^k can be thought of as a forcing term so that (54) is a periodically forced version of (47) with a family of periodic solutions

$$I_j^k = I_j^{k*} + \rho Z \quad (55)$$

that solve (54) where I_j^{k*} is a particular solution and ρ is a constant (also recall that Z is the gradient of the phase response curve evaluated on the periodic orbit). A normalization can be obtained by exploiting the relationships $\dot{\psi}_1 = \kappa_1 \psi_1 + \psi_2$ and $\dot{\psi}_2 = \kappa_2 \psi_2$. Recall from (19) that $\dot{\psi}_k = \frac{\partial \psi_k}{\partial t} \cdot \frac{dx}{dt}$. Noting that $\frac{dx}{dt}$ can be written as $F(x^\gamma) + \frac{d\Delta x}{dt}$ and using the expansion for $\frac{d\Delta x}{dt}$ given in (25), one can show that the equations of the form I_j^k must be normalized so that

$$\begin{aligned} \kappa_1 &= I_1^T DF(x^\gamma)g^1 + I_1^{1T} F(x^\gamma), \\ 1 &= I_1^T DF(x^\gamma)g^2 + I_1^{2T} F(x^\gamma), \\ 0 &= I_2^T DF(x^\gamma)g^1 + I_2^{1T} F(x^\gamma), \\ \kappa_1 &= I_2^T DF(x^\gamma)g^2 + I_2^{2T} F(x^\gamma). \end{aligned} \quad (56)$$

Note that the θ dependence on the terms of (56) is not written for notational convenience, but these conditions are valid for any choice of θ on the limit cycle.

B. Degenerate isostable reduced equations for fixed points

Section IV A illustrates phase and degenerate isostable reduction for periodic orbits for which the fundamental matrix has Jordan blocks of size larger than 1. When the attractor is a fixed point, x_0 , with a linearization that has an eigenvalue λ_1 with a Jordan block of size m , the following isostable reduction can be obtained:

$$\begin{aligned} \dot{\psi}_k &= \lambda_1 \psi_k + \psi_{k+1} + \mathcal{I}_k(\psi_1, \dots, \psi_m) \cdot u(t), \\ k &= 1, \dots, m-1, \\ \dot{\psi}_m &= \lambda_1 \psi_m + \mathcal{I}_m(\psi_1, \dots, \psi_m) \cdot u(t), \\ x &= x_0 + \mathcal{G}(\psi_1, \dots, \psi_m). \end{aligned} \quad (57)$$

Equation (57) assumes that all other eigenvalues λ_j with $j > m$ of the linearization about the fixed point are large in magnitude so that their components decay rapidly and can be ignored in the reduction. Notice the similarity in structure between (57) and (22) which are identical except for the fact that (57) does not have a phase coordinate. The terms \mathcal{I}_m and \mathcal{G} can be expanded

and computed in a similar manner to those from the reduction (57). Employing a similar approach that was used for the periodic case, expansion in powers of the degenerate isostable coordinates yields

$$\mathcal{G}(\psi_1, \dots, \psi_m) = \sum_{k=1}^m [\psi_k g^k] + \sum_{j=1}^m \sum_{k=1}^j [\psi_j \psi_k g^{jk}] + \sum_{i=1}^m \sum_{j=1}^i \sum_{k=1}^j [\psi_i \psi_j \psi_k g^{ijk}] + \dots, \quad (58)$$

$$\mathcal{I}_n(\psi_1, \dots, \psi_m) = I_n + \sum_{k=1}^m [\psi_k I_n^k] + \sum_{j=1}^m \sum_{k=1}^j [\psi_j \psi_k I_n^{jk}] + \sum_{i=1}^m \sum_{j=1}^i \sum_{k=1}^j [\psi_i \psi_j \psi_k I_n^{ijk}] + \dots \quad (59)$$

Compared to (23) and (37), the above terms of the expansion of the form $g^{ijk\dots}$ and $I_n^{ijk\dots}$ in the above equations are constant and do not depend on θ . For fixed-point attractors, degenerate isostable coordinates have the same unperturbed decay governed by relationships of the form (20) and (21). For this reason, the computation of the terms of the expansions (58) and (59) can be performed using a nearly identical strategy to the one presented in Sec. IV A. Because the strategy for computation of the individual terms of (58) and (59) is similar to the strategy for computing the terms of (23) and (37), respectively, only a brief discussion is given here emphasizing the important differences to consider when the attractor is a fixed point instead of a periodic orbit.

Computing the terms of \mathcal{G} and each \mathcal{I}_n

To begin, consider the terms of \mathcal{G} . Noting that $\mathcal{G} \approx \Delta x$ gives the dynamics on a hypersurface determined by the nonzero isostable coordinates, taking the time derivative of the unperturbed flow on this hypersurface yields

$$\frac{d\Delta x}{dt} = \sum_{k=1}^m [g^k (\psi_k \lambda_1 + \psi_{k+1})] + \sum_{j=1}^m \sum_{k=1}^j [2g^{jk} \psi_j \psi_k \lambda_1 + g^{jk} (\psi_j \psi_{k+1} + \psi_k \psi_{j+1})] + \dots \quad (60)$$

Notice that compared to (24), the time derivative of each $g^{ijk\dots}$ function is zero since the attractor is a fixed point (i.e., there is no phase coordinate). Taylor expanding (1) using Eq. (A3) from Appendix A yields an equation similar to (25),

$$\frac{d\Delta x}{dt} = DF(x_0) \left[\sum_{k=1}^m [\psi_k g^k] + \sum_{j=1}^m \sum_{k=1}^j [\psi_j \psi_k g^{jk}] + \dots \right] + Q_{\text{fp}}(\Delta x), \quad (61)$$

where

$$Q_{\text{fp}}(\Delta x) = \begin{bmatrix} \sum_{i=2}^{\infty} \frac{1}{i!} \left[\otimes \left[\sum_{k=1}^m [\psi_k g^k] + \sum_{j=1}^m \sum_{k=1}^j [\psi_j \psi_k g^{jk}] + \dots \right]^T \text{vec}(f_1^{(i)}) \right] \\ \vdots \\ \sum_{i=2}^{\infty} \frac{1}{i!} \left[\otimes \left[\sum_{k=1}^m [\psi_k g^k] + \sum_{j=1}^m \sum_{k=1}^j [\psi_j \psi_k g^{jk}] + \dots \right]^T \text{vec}(f_N^{(i)}) \right] \end{bmatrix}, \quad (62)$$

where all partial derivatives of (62) are evaluated at x_0 . Similarly to the strategy suggested in Sec. IV A 1 setting (60) and (61) equal to each other, one can obtain relationships between the terms of the expansion by matching the powers of the isostable coefficients.

Using this approach, when $m = 2$, the first order accurate equations are

$$0 = (DF - \lambda_1 \text{Id})g^1, \quad (63)$$

$$0 = (DF - \lambda_1 \text{Id})g^2 - g^1. \quad (64)$$

Compared to (42) and (43), the above equations are no longer time-varying and are simply sets of linear matrix equations. Note that (63) and (64) require normalization which can be accomplished by requiring $g^1 = P_1 [1 \ 0]^T$ and $g^2 = P_1 [0 \ 1]^T$ where P_1 was defined just before Eq. (8). Using a similar strategy to the one detailed in Sec. IV A 4, one can group the terms of $Q_{\text{fp}}(\Delta x)$ according to

$$Q_{\text{fp}}(\Delta x) = \sum_{j=1}^m \sum_{k=1}^j [\psi_j \psi_k Q_{\text{fp}}^{jk}] + \sum_{i=1}^m \sum_{j=1}^i \sum_{k=1}^j [\psi_i \psi_j \psi_k Q_{\text{fp}}^{ijk}] + \dots \quad (65)$$

With this definition, equations for the higher order terms of the expansion (58) are

$$\begin{aligned} 0 &= [DF - (\alpha + \beta)\lambda_1 \text{Id}]g_{12}^{\alpha\beta} + Q_{12}^{\alpha\beta}, \quad \text{for } \beta = 0, \\ 0 &= [DF - (\alpha + \beta)\lambda_1 \text{Id}]g_{12}^{\alpha\beta} + Q_{12}^{\alpha\beta} - (\alpha + 1)g_{11}^{\alpha+1, \beta-1}, \quad \text{for } \beta > 0, \end{aligned} \quad (66)$$

where the meaning of the notation $g^{\frac{\alpha\beta}{12}}$ was defined below Eq. (45). As with (63) and (64), each of the terms of the form $g^{\frac{\alpha\beta}{12}}$ from (66) can be found by solving an associated linear matrix equation.

The terms of each \mathcal{I}_n can be computed using a similar strategy to the one presented in Sec. IV A 3. By mirroring the arguments starting with Eq. (32) and ending with (36), noting that each $\frac{d\mathcal{I}_n}{dt} = 0$ since the attractor is now a fixed point, one finds

$$0 = -\left(\left.\frac{\partial F^T}{\partial x}\right|_{x_0} - \lambda_1 \text{Id}\right)\mathcal{I}_n + \mathcal{I}_{n+1},$$

$$n = 1, \dots, m-1. \quad (67)$$

A similar argument can be followed to find

$$0 = -\left(\left.\frac{\partial F^T}{\partial x}\right|_{x_0} - \lambda_1 \text{Id}\right)\mathcal{I}_m. \quad (68)$$

As illustrated in Sec. IV A 3, substituting (59) in for each \mathcal{I}_n , replacing $\left.\frac{\partial F^T}{\partial x}\right|_{x_0}$ by the expression (B1) from Appendix B, and matching powers of the isostable coefficients, relationships for the terms of the asymptotic expansions can be derived. For instance, when $m = 2$, one finds the relationships for the zeroth order terms

$$0 = -(DF - \lambda_1 \text{Id})I_1 + I_2, \quad (69)$$

$$0 = -(DF - \lambda_1 \text{Id})I_2, \quad (70)$$

which can be solved as a linear matrix equation. As is the case when working with periodic-orbit attractors, the solutions to (69) and (70) must be normalized according to $I_1^T g^1 = 1$ and $I_2^T g^2 = 1$. Additional relations can be obtained for the higher order terms with similar structure to (52) and (53).

C. Generalized degenerate isostable coordinates

Recent work [38,39], has proposed the use of an adaptive isostable coordinate reduced framework, whereby the nominal system parameters are allowed to change in order to keep the isostable coordinates small. This strategy is described in more detail in the example from Sec. VB and generally results in a more accurate reduced order model when compared to standard isostable reduction techniques. A fundamental requirement of the adaptive reduction framework is that the isostable coordinates are continuously differentiable with respect to system parameters; i.e., $\frac{\partial \psi_i}{\partial p}$ must exist and be continuous for all p . As illustrated in [38], this requires the isostable response curves to be continuous for all p .

The requirement that the isostable response curves be continuous with respect to parameter changes poses a problem if some parameters yield isostable coordinates that are degenerate; suddenly switching from the standard definition of isostable coordinates in Eq. (4) [resp., (7)] to (8) [resp., (13)] for a defective linearization will yield isostable coordinates that are not continuous. This problem can be mitigated by using generalized degenerate isostable coordinates as described here.

1. Generalized degenerate isostable coordinates of fixed-point attractors

Consider a fixed-point attractor x_0 of (1) with linearized, nondefective eigenvalues λ_1 and λ_2 where $\lambda_1 \neq \lambda_2$ with corresponding eigenvectors v_1 and v_2 . Because these eigenvalues are not defective, a standard definition of isostable coordinates is possible giving $\Psi = [\psi_1 \ \psi_2]^T$ with dynamics $\dot{\Psi} = \Lambda \Psi$ where Λ is a diagonal matrix with λ_1 and λ_2 on the diagonal. Generalized degenerate isostable coordinates can be defined

according to the transformation $\Psi^G = A^{-1}\Psi$,

$$A = \begin{bmatrix} \frac{1}{\alpha} & \frac{1}{\alpha(\lambda_1 - \lambda_2)} \\ 0 & -\frac{1}{\beta} \end{bmatrix}, \quad (71)$$

where $\Psi^G = [\psi_1^G \ \psi_2^G]^T$ are the generalized degenerate isostable coordinates, and α and β are any nonzero constant, these generalized degenerate isostable coordinates. With this transformation, one can verify that

$$\dot{\Psi}^G = J^G \Psi^G, \quad (72)$$

in the entire basin of attraction of the fixed point where

$$J^G = \begin{bmatrix} \lambda_1 & 1 \\ 0 & \lambda_2 \end{bmatrix}. \quad (73)$$

Many coordinate transformations are possible for which the dynamics mirror those of the degenerate isostable coordinates, but the main goal here is to identify a coordinate framework that yields isostable coordinates that are continuously differentiable with respect to the system parameters; as stated previously, this means that the isostable response curves need to be continuous with respect to parameter perturbations. To identify such a coordinate framework, consider the expansions

$$\mathcal{G}^G(\psi_1^G, \psi_2^G) = \psi_1^G g^1 + \psi_2^G g^2 + (\psi_1^G)^2 g^{11} + \psi_1^G \psi_2^G g^{12} + (\psi_2^G)^2 g^{22} + \dots, \quad (74)$$

$$\mathcal{I}_n^G(\psi_1^G, \psi_2^G) = I_n + \psi_1^G I_n^1 + \psi_2^G I_n^2 + (\psi_1^G)^2 I_n^{11} + \psi_1^G \psi_2^G I_n^{12} + (\psi_2^G)^2 I_n^{22} + \dots, \quad (75)$$

where $\Delta x = x_0 + \mathcal{G}^G(\psi_1^G, \psi_2^G)$ and $\frac{\partial \psi_n^G}{\partial x} = \mathcal{I}_n^G(\psi_1^G, \psi_2^G)$ for $n = 1, 2$. Equations (74) and (75) are similar in structure to the expansions (58) and (59), except that only two isostable

coordinates are considered here and that the unperturbed dynamics have the form (72). Following a similar approach to the one detailed in Sec. IV B 1 [i.e., taking the time derivative (74), comparing it to the Taylor expansion of (1), and matching powers of the isostable coordinates], one can find relationships that describe the terms of the expansion (74). For instance, the leading order terms of (74) are given by

$$0 = (DF - \lambda_1 \text{Id})g^1, \quad (76)$$

$$0 = (DF - \lambda_2 \text{Id})g^2 - g^1, \quad (77)$$

where, once again, DF denotes the Jacobian evaluated at x_0 . Comparing to (63) and (64), the above equations are identical except that the λ_1 has been replaced by a λ_2 in (77). Because both $(DF - \lambda_1)$ and $(DF - \lambda_2)$ from (76) and (77) have nonempty null spaces, there is some freedom in the choice of g^1 and g^2 [as expected from the fact that A from (71) is not unique]. One can verify that the choice

$$\begin{aligned} g^1 &= v_1, \\ g^2 &= (DF - \lambda_2 \text{Id})^\dagger v_1, \end{aligned} \quad (78)$$

where \dagger denotes the Moore-Penrose pseudoinverse, satisfies both (76) and (77). Here, g^1 is an eigenvector of DF with eigenvalue λ_1 so that (76) follows immediately. To see that this choice of g^2 satisfies (77), note that g^1 is also an eigenvector of $(DF - \lambda_2 \text{Id})$. With this in mind, $(DF)(DF)^\dagger g^1 = g^1$ and (77) follows immediately. Relationships that characterize the higher order terms can also be found by using a strategy similar to the one used to yield the relationships (66).

The choice of g^1 and g^2 from (78) is meant to mirror a strategy that one can use to find the matrix P_1 for the defective linearization from the definition of degenerate isostable coordinates from (8): for a defective eigenvalue λ_1 of DF , the first column of P_1 can be chosen to be the corresponding eigenvalue, v_1 , and the second column of P_1 can be taken to be the generalized eigenvector $(DF - \lambda_1 \text{Id})^\dagger v_1$. As such, provided DF , λ_1 , λ_2 , and v_1 change continuously with respect to parameter changes, this strategy can be used to find g^1 and g^2 that vary continuously with changing parameters in situations where some parameters yield defective linearizations.

The terms of each \mathcal{I}_n from (75) can also be found using a strategy similar to the one employed in Sec. IV B 1. With this approach, one finds that

$$0 = -(DF^T - \lambda_1 \text{Id})I_1 + I_2, \quad (79)$$

$$0 = -(DF^T - \lambda_2 \text{Id})I_2. \quad (80)$$

Once again, (79) and (80) only differ from Eqs. (69) and (70) in that λ_1 is replaced by λ_2 in (80). As before, the normalization $I_1^T g^1 = 1$ and $I_2^T g^2 = 1$ uniquely determines I_1 and I_2 .

Computing the terms of \mathcal{I}_1^G and \mathcal{I}_2^G , one can obtain a set of reduced order equations

$$\begin{aligned} \dot{\psi}_2^G &= \lambda_1 \psi_1^G + \psi_2^G + \mathcal{I}_1^G(\psi_1^G, \psi_2^G) \cdot u(t), \\ \dot{\psi}_1^G &= \lambda_2 \psi_2^G + \mathcal{I}_2^G(\psi_1^G, \psi_2^G) \cdot u(t), \\ x &= x_0 + \mathcal{G}(\psi_1^G, \psi_2^G). \end{aligned} \quad (81)$$

Note that Eq. (81) only differs in structure from (57) in that the eigenvalue λ_2 appears in the second equation. This

generalized degenerate isostable reduced framework will be employed in the example from Sec. VB.

2. Generalized degenerate isostable coordinates of periodic orbit attractors

The notion of generalized degenerate isostable coordinates can also be used for systems that have stable periodic orbits instead of stable fixed points. Consider a stable T -periodic attractor $x^\gamma(t)$ of (1), with nondefective Floquet multipliers κ_1 and κ_2 where $\kappa_1 \neq \kappa_2$. Because these eigenvalues are not defective, standard isostable coordinates can be defined with $\Psi = [\psi_1 \ \psi_2]^T$ that have dynamics $\dot{\Psi} = \Lambda \Psi$ where Λ is a diagonal matrix with κ_1 and κ_2 on the diagonal. Generalized degenerate isostable coordinates can be defined according to the transformation $\Psi^G = [\psi_1^G \ \psi_2^G]^T = A^{-1}\Psi$, where A was defined in (71). As with generalized isostable coordinates of fixed-point attractors, these generalized isostable coordinates have unperturbed dynamics $\dot{\Psi}^G = J^G \Psi^G$ in the basin of attraction of the limit cycle where J^G has the same form as (73) (except with the λ_1 and λ_2 replaced by κ_1 and κ_2 , respectively).

As in the fixed-point case, generalized degenerate isostable coordinates can be used in an adaptive isostable reduced framework where it is necessary to define a coordinate system that is continuously differentiable with respect to the allowable parameters. This can be accomplished using a strategy that is similar to the case where the attractor is a fixed point, and details are omitted here.

D. Degenerate isostable coordinates defined using the slowest decaying Koopman eigenfunction associated with a defective linearization

In [11], a degenerate isostable coordinate definition was suggested to characterize only the slowest decaying Koopman eigenfunctions associated with a defective linearization. This alternative degenerate isostable coordinate definition is investigated here with emphasis given to its resulting reduced order models. As discussed in the example in Sec. VA to follow, this definition is typically not sufficient for reduced order modeling purposes.

1. Slowest decaying degenerate isostable coordinates for fixed points

Suppose that (1) has a fixed-point attractor x_0 . As suggested in [11], if its linearization from (2) has a size m Jordan block with corresponding eigenvalue λ_1 , one can replace $\exp(-\lambda_1 t)$ by $t^{1-m} \exp(-\lambda_1 t)$ in the definition of isostable coordinates from (3). Recall that λ_1 is defined so that $|\text{Re}(\lambda_1)| \leq |\text{Re}(\lambda_k)|$ for all $k > 1$. Once again, the unperturbed flow $\phi(t, x)$ of (1) (i.e., the solution when $u = 0$) will be considered. Using the approach suggested by [11] and drawing on the definitions provided in Sec. III A, the following isostable coordinate definition can be formulated:

$$\psi_1^s(x) = (m-1)! \lim_{t \rightarrow \infty} [e_1^T W_1^T (\phi(t, x) - x_0) \exp(-\lambda_1 t) t^{1-m}], \quad (82)$$

where W_1 was defined above (8) and e_1 is the first element of the standard unit basis. Note that similarly to the definition (8),

the above definition does not use Laplace averages and simply takes the isostable coordinate in the infinite time limit. Recalling from (9) that in the infinite time limit, $\phi(t, x) - x_0 \approx P_1 \exp(J_1 t) S_0(x)$ and that $W_1^T P_1 = \text{Id}$, one can simplify (82) as

$$\begin{aligned} \psi_1^s(x) &= (m-1)! \lim_{t \rightarrow \infty} \left\{ \exp(\lambda_1 t) \left[1 \quad t \quad \dots \quad \frac{t^{m-1}}{(m-1)!} \right] \right. \\ &\quad \left. \times S_0(x) \exp(-\lambda_1 t) t^{1-m} \right\} \\ &= e_m^T S_0(x). \end{aligned} \quad (83)$$

Recalling the relationship (10) from Sec. III A, one finds that ψ_1^s is identically equal to ψ_m that results when using the definition (8). From (16) one finds that $\dot{\psi}_m = \lambda_1 \psi_m$, so that

$$\frac{d\psi_1^s}{dt} = \lambda_1 \psi_1^s. \quad (84)$$

Alternatively, it is also possible to derive Eq. (84) directly from the definition (83). A reduced order model for (1) follows from the equivalence between ψ_1^s and ψ_m :

$$\begin{aligned} \dot{\psi}_1^s &= \lambda_1 \psi_1^s + I_m \cdot u(t), \\ x &= x_0 + g^m \psi_1^s, \end{aligned} \quad (85)$$

where g^m and I_m are taken from the terms of the expansions from (58) and (59), respectively. Note that the reduced equations (85) only include the lowest order terms in ψ_1^s .

2. Slowest decaying degenerate isostable coordinates for periodic orbits

Considering the solution of (1) when $u = 0$, suppose that the limiting behavior is a T -periodic orbit, $x^\gamma(t)$. Suppose also that the fundamental matrix of the linearization (6) has an eigenvalue λ_1 with associated size m Jordan block with $\kappa_1 = \ln(\lambda_1)/T$. Recall that κ_1 is defined so that $|\text{Re}(\kappa_1)| \leq |\text{Re}(\kappa_k)|$ for all $k > 1$. Similarly to the previous section, an extra term can be added to (7) to define a single isostable coordinate

$$\begin{aligned} \psi_1^s(x) &= (m-1)! \lim_{k \rightarrow \infty} \left[e_1^T W_1^T \left(\phi(t_\Gamma^k, x) - x_0^\Gamma \right) \right. \\ &\quad \left. \times \exp\left(-\kappa_1 t_\Gamma^k\right) \left(t_\Gamma^k\right)^{1-m} \right], \end{aligned} \quad (86)$$

where t_Γ^k and x_0^Γ were defined below (7). Recalling from (14) that as time approaches infinity, $\phi(t_\Gamma^k, x) - x_0^\Gamma \approx P_1 \exp(J_1 t_\Gamma^k) S_0^\Gamma(x)$ in addition to the relationship $W_1 P_1 = \text{Id}$, one can simplify (86) to

$$\begin{aligned} \psi_1^s(x) &= (m-1)! \lim_{k \rightarrow \infty} \left\{ \exp(\kappa_1 t_\Gamma^k) \left[1 \quad t_\Gamma^k \quad \dots \quad \frac{(t_\Gamma^k)^{m-1}}{(m-1)!} \right] \right. \\ &\quad \left. \times S_0^\Gamma(x) \exp(-\kappa_1 t_\Gamma^k) \left(t_\Gamma^k\right)^{1-m} \right\} \\ &= e_m^T S_0^\Gamma(x). \end{aligned} \quad (87)$$

Comparing to Eq. (15) which is valid for isostable coordinates defined according to (13), one finds that $\psi_1^s(x) = \psi_m$. Drawing on this equivalence, and considering the unperturbed decay of ψ_m from (18),

$$\frac{d\psi_1^s}{dt} = \kappa_1 \psi_1^s. \quad (88)$$

Additionally, a reduced order model can be obtained,

$$\dot{\theta} = \omega + Z(\theta) \cdot u(t),$$

$$\begin{aligned} \dot{\psi}_1^s &= \kappa_1 \psi_1^s + I_m(\theta) \cdot u(t), \\ x &= x^\gamma(\theta) + g^m(\theta) \psi_1^s, \end{aligned} \quad (89)$$

where $g^m(\theta)$, $Z(\theta)$, and $I_m(\theta)$ are taken directly from the terms of the expansions (23), (28), and (37), respectively. Once again, only the lowest order terms in ψ_1^s are kept in the reduction (89).

3. A caution against using only a single degenerate isostable coordinate for reduced order modeling purposes

Definitions (82) and (86) characterize the absolute slowest components of the decay to the attractor. In some situations, a single isostable coordinate is enough to capture the essential information about the decay toward an attractor [12,13,27]. This usually requires the gap between $|\text{Re}(\lambda_1)|$ and $|\text{Re}(\lambda_2)|$ to be large enough to ensure a fast decay of the neglected isostable coordinates. When defining a single isostable coordinate associated with a size m Jordan block according to either (82) or (86), this necessary gap does not exist and $m-1$ coordinates with the same exponential decay rate are neglected from the resulting reduction. For this reason, reduced order models of the form (85) and (89) are generally insufficient to capture the full model behavior as will be illustrated in the examples to follow. Instead, the definitions (8) and (13) that define m isostable coordinates associated with a size m Jordan block are generally better.

V. EXAMPLES

A. Reduction of an entrained circadian oscillator

As a preliminary example, a model of an entrained oscillatory dynamical system will be considered that is often used to model circadian oscillations [40]:

$$\begin{aligned} \dot{a} &= h_1 \frac{K_1^n}{K_1^n + c^n} - h_2 \frac{a}{K_2 + a} + L(t_s), \\ \dot{b} &= h_3 a - h_4 \frac{b}{K_4 + b}, \\ \dot{c} &= h_5 b - h_6 \frac{c}{K_6 + c}, \\ \dot{t}_s &= 1 + t_{\text{shift}}(t). \end{aligned} \quad (90)$$

The model (90) is similar to the Goodwin model [41] and describes the fundamental mechanism for self-sustained oscillations in circadian clock genes: the variable a represents the concentration of a clock gene, b is the concentration of the resulting protein, and c is the concentration of the active protein. The parameter $t_s \in \mathbb{S}^1$ is a timelike variable in the range $[0, 24)$ that governs a 24-hour external light-dark cycle,

$$L(t_s) = L_a \left[\frac{1}{1 + \exp[-2(t_s - 6)]} - \frac{1}{1 + \exp[-2(t_s - 18)]} \right], \quad (91)$$

where L_a is the maximum amplitude of the applied light. The term $t_{\text{shift}}(t)$ is used to incorporate time shifts into the model as would occur, for instance, from rapid eastward or westward travel. Putting (90) in the form of (1), $x = [a \quad b \quad c \quad t_s]^T$ is the state, $u(t) = [0 \quad 0 \quad 0 \quad t_{\text{shift}}]^T$

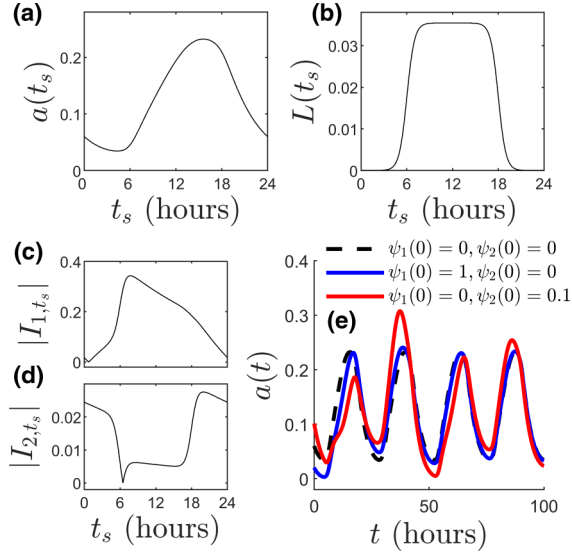


FIG. 1. Panel (a) shows a trace of $a(t_s)$ on the periodic orbit of (90). The corresponding light-dark cycle is shown in panel (b). The chosen parameter set results in a fundamental matrix with a defective eigenvalue so that degenerate isostable coordinates must be used. The magnitudes of the isostable response curves computed on the periodic orbit (i.e., for the response curves computed to zeroth order accuracy in the isostable coordinates) are plotted for perturbations to t_s in panels (c) and (d). Traces of reduced order model outputs are shown in panel (e) with \mathcal{G} computed to first order accuracy in the isostable coordinates. The dashed line takes the initial isostable coordinates to be zero yielding the entrained periodic orbit. Blue and red lines show model outputs for different initial isostable coordinates giving a sense of the decay rates of transients.

is taken to be the external perturbation, and the remaining terms are contained in $F(x)$. Parameters are taken to be $n = 4, h_1 = 0.67, h_2 = 0.34, h_3 = 0.7, h_4 = 0.35, h_5 = 0.7, h_6 = 0.35, K_1 = 1, K_2 = 1, K_4 = 1,$ and $K_6 = 1$. When $L(t_s) = 0$, (90) has a stable 24.15-hour periodic orbit. For all but the smallest nonzero values of L_a , the model becomes entrained to the 24-hour light-dark cycle. Note here that t_s is explicitly included in the state of (90) so that the entrained periodic orbit is autonomous and can be viewed as a limit-cycle oscillator. Recalling that the definition of isochrons from (5) characterizes the infinite time behavior and that the limiting behavior is solely dependent on t_s , one can show that when L_s is large enough to cause entrainment, the asymptotic phase of (90) is simply given by $\theta = 2\pi t_s/24$. As such, isostable coordinates must be used to study transient behaviors such as reentrainment and to characterize the influence of perturbations on (90).

Equation (90) will be studied taking $L_a = 3.545 \times 10^{-2}$. For this value of L_a , the slowest decaying Floquet multiplier of the fundamental matrix is $\lambda_1 = -0.44$. This eigenvalue is defective, with algebraic multiplicity 2 and geometric multiplicity 1. The remaining nonunity Floquet multiplier is close to zero and will be ignored from the reduction. Degenerate isostable coordinates will be used to define a reduced order model of the form (22) to characterize perturbations applied to (90). Following the strategy discussed in Sec. IV A 4, the reduced order model is found by computing the necessary terms

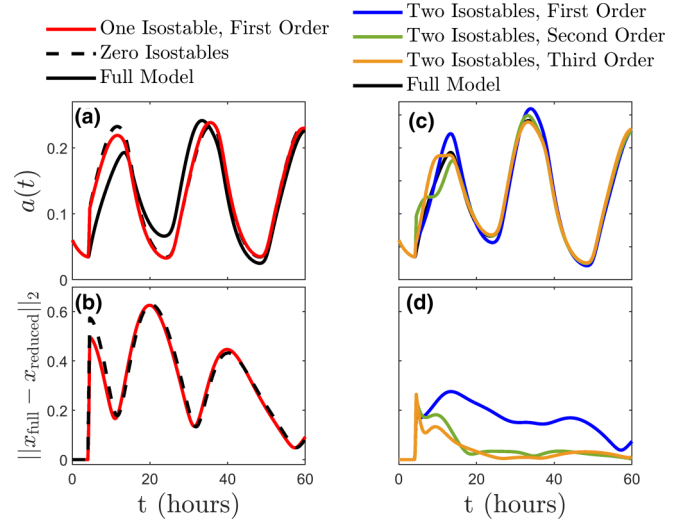


FIG. 2. Panels (a) and (c) show traces of $a(t)$ resulting from a sudden time advance of 4 hours when using various reduced order models. Panels (b) and (d) show the two-norm, $\|x\|_2 = (x^T x)^{1/2}$, of the difference between the full and reduced order models. Note that because the phase dynamics are known exactly, the errors in panels (b) and (d) approach 0 for all models as time goes to infinity.

of $\mathcal{G}(\theta, \psi_1, \psi_2)$, $\mathcal{I}_1(\theta, \psi_1, \psi_2)$, and $\mathcal{I}_2(\theta, \psi_1, \psi_2)$. Because of the simple relationship between t_s and phase discussed earlier, an exact relationship for the phase response curve $Z(\theta, \psi_1, \psi_2) = [0 \ 0 \ 0 \ 2\pi/24]^T$ can be obtained. Relevant features of the reduced order models are shown in Fig. 1. Panel (a) shows a trace of $a(t_s)$ over one cycle with $L(t_s)$ shown in panel (b). The magnitudes of $I_1(t_s)$ and $I_2(t_s)$ (i.e., the gradient of the isostable response curves evaluated on the periodic orbit) are shown in panels (c) and (d), respectively, for shifts in t_s . Note that the Floquet multipliers are negative yielding complex-valued Floquet exponents, isostable coordinates, and response curves. Panel (e) shows the model output for various initial isostable coordinates with \mathcal{G} computed to first order accuracy in ψ_1 and ψ_2 .

As suggested by [11], a single isostable coordinate can be defined according to (86) that characterizes the slowest decaying terms associated with the size 2 Jordan block. As shown in Sec. IV D 1, this results in a reduced order model of the form (89). The accuracy of various reduced order models is considered with results shown in Fig. 2 using an input $t_{\text{shift}} = 8$ lasting 0.5 hours, which corresponds to an overall 4-hour time advance. Panels (a) and (b) compare this single isostable reduced order model to both the full model simulations and a model that does not use isostable coordinates (where the output is simply the periodic orbit as a function of θ). For this application, a single isostable coordinate performs poorly and is not much better than simply assuming the state is on the periodic orbit at all times. Panels (c) and (d) compare reduced models of the form (22) that use each of the degenerate isostable coordinates. By convention, $u(t)$ is usually assumed to be an $O(\epsilon)$ term where ϵ is small. Under this assumption, one can show that both ψ_1 and ψ_2 are $O(\epsilon)$ terms using strategies similar to those employed in [42]. Accordingly, the j th order accurate (in ϵ) model

takes $\mathcal{I}_1(\theta, \psi_1, \psi_2)$ and $\mathcal{I}_2(\theta, \psi_1, \psi_2)$ up to $(j-1)$ th order accuracy in the isostable coordinates and $\mathcal{G}(\theta, \psi_1, \psi_2)$ up to j th order accuracy in the isostable coordinates. Compared to the single isostable reduced model, the two isostable model performs significantly better. Additionally, better agreement between the reduced and full models is observed as the order of accuracy increases.

B. Fitting a nonlinear partial differential equation to a model with degenerate isostable coordinates

A second example is considered here where the dynamics of a nonlinear partial differential equation are represented using an isostable reduced framework. The following reduction strategy allows the nominal boundary conditions to change and requires the isostable coordinates to be continuously differentiable with respect to the boundary conditions. As observed below, some parameter sets result in defective linearization. Consequently, in order to satisfy the continuity requirements, the use of degenerate isostable coordinates from Sec. IV C is necessary.

The model considered here will be the nonlinear Burgers equation, which is often used as a test bed for control and reduction techniques involving fluid flows because it has a convective nonlinearity that is similar to the Navier-Stokes equations. Specifically, the one-dimensional Burgers equation will be considered:

$$\frac{\partial w}{\partial t} = \frac{1}{\text{Re}} \frac{\partial^2 w}{\partial x^2} - w \frac{\partial w}{\partial x}, \quad (92)$$

where $x \in [0, 1]$ is the domain, Re is a viscosity term analogous to the Reynolds number from the Navier-Stokes equation, and $w_L(t)$ and $w_R(t)$ represent time-varying left and right boundary conditions at $x = 0$ and $x = 1$, respectively. In recent work [39], a model reduction framework was suggested for (92) that can be implemented with knowledge of the underlying dynamical equations. Here, a different approach will be taken, where an adaptive isostable reduced model is fitted to model outputs without any *a priori* knowledge of Eq. (92).

To accomplish this task, the notion of an adaptive phase and isostable reduction will be used which has been recently introduced in [38] and [39]. Following the formulation in [39], the partial differential equation (92) can be written as

$$\frac{\partial w}{\partial t} = F(w(x, t), p(t)), \quad (93)$$

where F gives the dynamics as a function of the state w and the time-varying boundary conditions $p = [w_L(t) \quad w_R(t)]^T$. Suppose that for all $p \in \Omega_p$ (where Ω_p is the set of all allowable parameters) the limiting behavior tends toward a steady state solution $w_{SS}(x, p)$. Output data from (93) will be fitted to an adaptive isostable reduced model of the form

$$\begin{aligned} \dot{\Psi}^G &= J^G(p)\Psi + B(p)\dot{p}, \\ w(x, t) &= w_{SS}(x, p) + \sum_{j=1}^{\sigma} \eta_j(x, p)\psi_j^G, \end{aligned} \quad (94)$$

where $\Psi^G = [\psi_1^G \quad \dots \quad \psi_{\sigma}^G]$ are a collection of generalized degenerate isostable coordinates, $J^G(p) \in \mathbb{R}^{\sigma \times \sigma}$ gives the unperturbed decay, $B(p) \in \mathbb{R}^{\sigma \times 2}$ characterizes the influence of

changes to the boundary conditions, and each $\eta_j(x, p)$ characterizes the deviation from the stationary solution as the isostable coordinates change. A similar reduced model of the form (94) that used nondegenerate isostable coordinates was investigated in [39] for the one-dimensional Burgers equation (92) and identified with knowledge of the full model equations (92); here it is assumed that the equations are not available and measurements of the model output will be used to identify the necessary terms of (94) instead.

1. Fitting a reduced order model to data from numerical simulations

Model output from (92) will be used to identify a reduced order model of the form (94). The necessary steps are given below. This procedure does not require knowledge of the underlying model and could also be applied to identify a reduced order model for a general system.

Step 1: For some choice of $p = [w_L \quad w_R]^T \in \Omega_p$, boundary conditions are set to $w|_{x=0} = w_L + \Delta w_L$ and $w|_{x=1} = w_R + \Delta w_R$ where both Δw_L and Δw_R are small. Simulation is performed long enough for the system to approach its steady state solution. The boundary conditions are then set to p , and (93) is simulated long enough so that the state approaches the new stationary solution. This is repeated for various choices of Δw_L and Δw_R to ensure that all relevant modes associated with the stationary solution $w_{SS}(x, p)$ are excited.

Step 2: For each simulation from step 1, finite-dimensional snapshots of $w(x, t)$ are taken and stored as $\hat{w}(x, t) \in \mathbb{R}^a$. The value $\hat{w}_{SS}(x, p)$ (a finite dimensional version of w_{SS}) is subtracted from each snapshot. The mean-subtracted snapshots are arranged in a matrix $Y \in \mathbb{R}^{a,b}$, where b is the number of snapshots taken. Proper orthogonal decomposition (POD) [43,44] is performed on the snapshots by taking the eigenvalues and eigenvectors (denoted by λ_j^{POD} and ξ_j , respectively) of the matrix YY^T . Here, the two most dominant POD modes are considered (i.e., the eigenvectors ξ_j with the largest associated eigenvalues λ_j^{POD}) and the rest are truncated. For each choice of p allowed for the model (92), only two POD modes are required to give a good representation of the local dynamics of solutions near $w_{SS}(x, p)$, i.e., $\sum_{j=1}^2 \lambda_j^{\text{POD}} / \sum_{j=1}^a \lambda_j^{\text{POD}} \approx 1$.

Step 3: For a given choice of p , coefficients $\mu(t) = [m_1(t) \quad m_2(t)]^T$ of the POD basis corresponding to a given time step can be calculated according to

$$m_j(t) = \xi_j^T(x, p)[\hat{w}(x, t) - \hat{w}_{SS}(x, p)]. \quad (95)$$

Taking $\Delta t = 0.05$ time unit intervals, a least-squares fitting strategy is used to infer the relationship $\mu(t + \Delta t) = A\mu(t)$. This is accomplished as in [20] by taking d pairs of measurements, arranging into the matrices $B_1 = [\mu(t_1) \quad \dots \quad \mu(t_d)]$ and $B_2 = [\mu(t_1 + \Delta t) \quad \dots \quad \mu(t_d + \Delta t)]$, and taking $A = B_2 B_1^{\dagger}$ where \dagger denotes the pseudoinverse. The matrix A is a least-squares fit of the mapping from one state to the next with Δt time unit intervals. A continuous time relationship can be obtained yielding the dynamics in the POD coordinate

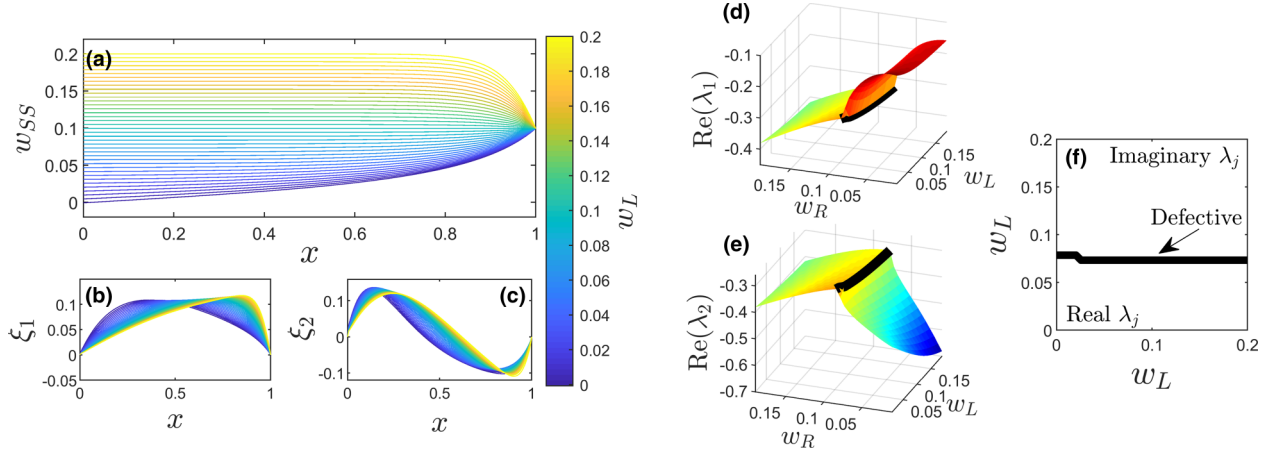


FIG. 3. POD reduced models resulting from completing steps 1 through 3 of the procedure given in Sec. V B 1. Panel (a) shows the steady state solutions that result when taking $w_R = 0.1$ with various values of w_L . Panels (b) and (c) show the principal POD modes. Panels (d) and (e) show the eigenvalues of $\hat{A}(p)$ associated with the reduced POD model from (96) with the black line highlighting values for which \hat{A} is defective. Panel (f) highlights the parameter sets for which \hat{A} is defective. Because some parameters require the use of degenerate isostable coordinates, generalized defective isostable coordinate system must be used for the reduced equations (94) to ensure that the isostable coordinates are continuously differentiable with respect to w_L and w_R .

basis

$$\begin{aligned} \dot{\mu} &= \hat{A}(p)\mu, \\ \hat{w}(x, t) &= \hat{w}_{SS}(x, p) + \sum_{j=1}^2 \xi_j(x, p)m_j(t), \end{aligned} \quad (96)$$

where $\hat{A} = \ln(A)/\Delta t$.

Step 4: Steps 1 through 3 are repeated over various values of $p \in \Omega_p$. The resulting information is shown in Fig. 3. Panel (a) shows the steady state solution for various boundary conditions. Panels (b) and (c) show the corresponding principal POD modes. Panels (d) and (e) show the principal eigenvalues of $\hat{A}(p)$ obtained from the fitting strategy from step 3. Panel (f) highlights the boundary over which the eigenvalues transition between real and imaginary values. At this boundary, the matrix \hat{A} is defective. Ultimately, the goal is to obtain a reduced order model of the form (94) that captures the dynamics of the full model (92); the use of generalized degenerate isostable coordinates is necessary because the matrix \hat{A} is defective for some values of p . For all choices of p , the POD basis is converted to a generalized degenerate isostable basis by defining $Q = [v_1 \quad (\hat{A} - \lambda_2 \text{Id})^\dagger v_1]$, where v_1 and v_2 are eigenvectors of \hat{A} associated with eigenvalues λ_1 and λ_2 , respectively. As described by Eq. (78), this choice of Q ensures the coordinate transform $\mu = Q\Psi^G$ has the dynamics $\dot{\Psi}^G = J^G(p)\Psi^G$ where $J^G(p) = Q^{-1}\hat{A}Q$ has the same form as (73). These generalized degenerate isostable coordinates can be defined in this manner regardless of whether \hat{A} is defective or not. For each choice of p , one can apply the appropriate coordinate transformation to the POD-based model of the form (96). Comparing the result to the desired model of the form (94), one finds the relationships

$$[\eta_1(x, p) \quad \eta_2(x, p)] = [\xi_1(x, p) \quad \xi_2(x, p)]Q. \quad (97)$$

Additionally, considering the relationship (95), for states close to the stationary solution, one finds

$$\begin{aligned} \Psi^G(t) &= \begin{bmatrix} \psi_1^G(t) \\ \psi_2^G(t) \end{bmatrix} = Q^{-1}[\xi_1(x, p) \quad \xi_2(x, p)]^T \\ &\quad \times [\hat{w}(t, x) - \hat{w}_{SS}(x, p)]. \end{aligned} \quad (98)$$

After completing step 4, all information about (94) is known except for $B(p)$.

Step 5: The terms of

$$B(p) = \begin{bmatrix} B_1^L(p) & B_1^R(p) \\ B_2^L(p) & B_2^R(p) \end{bmatrix} \quad (99)$$

must be fitted to the model output. Above, the notation B_1^L , for instance, characterizes the shift in the first generalized degenerate isostable coordinate resulting from a change in the parameter w_L . For a given choice of $p = [w_L \quad w_R]^T$, the terms of $B_1^L(p)$ and $B_1^R(p)$ can be fitted by first taking $w|_{x=0} = w_L + \Delta w_L$ and $w|_{x=1} = w_R$ and allowing the system to come to steady state. Here, Δw_L is assumed to be small. At $t = t_1$, boundary conditions are set to p , (i.e., w_L is shifted by $-\Delta w_L$) and the value of Ψ^G at $t = t_1 + \Delta t$ is inferred using the relationship (98). Subsequently, the value of Ψ^G at $t = t_1$ can be inferred according to $\Psi^G(t_1) = \exp[-J^G(p)\Delta t]\Psi^G(t_1 + \Delta t)$. Assuming that this shift in isostable was entirely due to the shift in w_L , one finds the approximation $[B_1^L(p) \quad B_2^L(p)]^T \approx -\Psi^G(t_1)/\Delta w_L$. These measurements are repeated taking different values of Δw_L to obtain a good approximation of $[B_1^L(p) \quad B_2^L(p)]$. Panel (a) of Fig. 4 shows a pictorial representation of the strategy used to infer B_1^L and B_2^L .

Step 6: Step 5 is repeated for various choices of $p \in \Omega_p$.

Step 7: Steps 5 and 6 are repeated with small shifts to w_R instead of w_L in order to estimate the remaining terms of the matrix $B(p)$. The real components of $B(p)$ that are inferred as part of steps 5–7 are shown in panels (b)–(e) of Fig. 4.

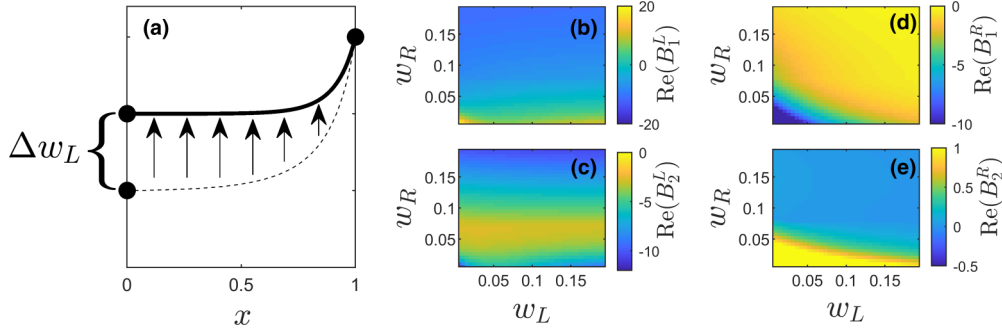


FIG. 4. Panel (a) shows a visual representation of the procedure used to infer B_1^L and B_2^L . For the given boundary conditions of $p = [w_L \ w_R]^T$, one can take $w_L|_{x=0} = w_L + \Delta w_L$ until the steady state simulation represented by the dotted line is achieved. Boundary conditions are then set to p and the decay to the new steady state (black line) is used to infer the change in the generalized degenerate isostable coordinate as described in step 5. This process is repeated for multiple values of p and for perturbations to w_R in order to infer the terms of $B(p)$. The real components of the resulting inferred functions for the model (92) are shown in panels (b)–(e).

2. Comparison between full and reduced model simulations

After completing the steps detailed in Sec. V B 1, the resulting model (94) is compared to full model simulations of (92) with results shown in Fig. 5. Left and right boundary conditions are taken to vary sinusoidally as shown in panel (a), and simulations are performed from an initial condition of $w(x, 0) = 0.1$. For simulations of the reduced order model (94), the resulting isostable coordinates as a function of time are shown in panel (b). The blue curve in panel (c) shows the two norm ($\|w\|_2 \equiv [\int_0^1 w^2(x) dx]^{1/2}$) of the error between the

full and reduced order solutions given by (92) and (94), respectively. The red curve shows the error between a model that neglects all isostable coordinates so that $w(x, t) = w_{SS}(p, x)$. Individual profiles of each of these model outputs are shown in panels (d) and (e) at $t = 70$ and $t = 120$ units, respectively. Inclusion of the isostable coordinate dynamics is essential for replicating the output of the full model equations.

VI. DISCUSSION AND CONCLUSIONS

Istable reduction provides a powerful strategy to obtain low-order models that replicate the behaviors of a dynamical system with a fixed-point or periodic-orbit attractor [11, 14, 17, 20–22]. Existing reduction strategies that use isostable coordinates focus almost exclusively on nondegenerate isostable coordinates that are associated with eigenvalues (or Floquet multipliers) with equal algebraic and geometric multiplicities. In this work, an extension of the isostable coordinate framework is proposed that can be used to characterize the decay of Koopman eigenfunctions associated with a defective eigenvalue, i.e., an eigenvalue associated with a size $m > 1$ Jordan block. Separate definitions are provided for systems with fixed-point attractors (8) and limit-cycle attractors (13). These degenerate isostable coordinates inherit many of the properties of their nondegenerate counterparts; most importantly, in the entire basin of attraction of their associated attractors, unperturbed dynamics of degenerate isostables have a relatively simple decay that allows for the computation of the necessary terms of reduced order models as discussed in Sec. IV.

While this work has considered reduced order systems that contain only degenerate isostable coordinates (after the fast decaying isostable coordinates are truncated), it would be relatively straightforward to adapt the techniques presented in this work to include systems that contain a mixture of both degenerate and nondegenerate isostable coordinates. Because the unperturbed dynamics of isostable coordinates associated with different Jordan blocks are decoupled from each other, mixtures of degenerate and nondegenerate isostable coordinates can be readily considered (this is the same feature that allows for the truncation of the rapidly decaying terms).

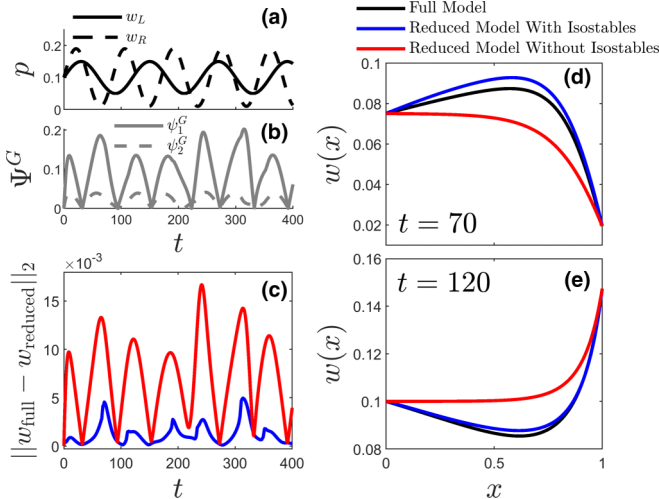


FIG. 5. Comparisons are shown between full and reduced order models from (92) and (94), respectively. Panel (a) shows the applied sinusoidally varying boundary conditions. Panel (b) shows the resulting generalized degenerate isostable coordinates of the reduced order model. Panel (c) shows the error between the full and reduced order models as a function of time in blue. The red curve shows the error between the full model and a model that only considers the steady state, i.e., by setting all isostable coordinates to zero for all time so that $w(x, t) = w_{SS}(x, p)$. Panels (d) and (e) show individual profiles of $w(x)$ for different times. These times are specifically chosen to highlight the worst-case performance of the reduced order models. The inclusion of the isostable coordinate dynamics is essential for replicating the output of the full model equations.

From a statistical perspective (i.e., when choosing a matrix at random) defective eigenvalues are rare. At first glance, one might have the impression that degenerate isostable coordinates would be of little practical utility. However, as illustrated in Sec. VB, when using an adaptive isostable reduction technique that allows for the nominal system parameters to change, if any allowable system parameters yield a linearized system with a defective eigenvalue, the degenerate isostable reduction framework must be used so that the resulting isostable coordinates are continuously differentiable with respect to the allowable parameters. For this reason, degenerate isostable coordinates will likely find practical utility in adaptive reduction frameworks such as the ones used in this work and in [38] and [39]. Additionally, in an experimental setting where noise is unavoidable, it may be difficult to implement standard isostable reduction techniques on a system with a nearly defective eigenvalue and the use of generalized degenerate isostable coordinates as discussed in Sec. IV C would likely confer robustness to the reduction methodology. Finally, engineered systems are usually designed using structure and symmetries that can make defective linearizations more likely and would necessitate the use of defective isostable coordinates proposed here.

ACKNOWLEDGMENT

This material is based on work supported by National Science Foundation Grants No. CMMI-1933583 and No. CMMI-2024111.

APPENDIX A: ASYMPTOTIC EXPANSION OF VECTOR VALUED FUNCTIONS

Using a strategy given in [21], an asymptotic expansion of $F(x)$ from (1) centered at x can be obtained as follows. Let $F(x) = [f_1 \dots f_N]^T$. The same notation from [45] will be used with \otimes denoting the Kronecker product and $\text{vec}(\cdot)$ denoting a matrix operator that stacks the columns of a matrix into a single column vector. Defining $f_i^{(0)}(x)$ to be equal to f_j evaluated at x , a set of matrices containing partial derivatives of $f_i(x)$ will be defined recursively,

$$f_j^{(k)}(x) = \frac{\partial \text{vec}(f_j^{(k-1)})}{\partial x^T} \in \mathbb{R}^{N^{(k-1)} \times N}, \quad (\text{A1})$$

with all partial derivatives evaluated at x . Equation (A1) can be combined with the relationship $\text{vec}(ABC) = (C^T \otimes A)\text{vec}(B)$ [45] to yield the Taylor expansion

$$f_j(x + \Delta x) = f_j(x) + f_j^{(1)}(x)\Delta x + \sum_{i=2}^{\infty} \frac{1}{i!} [\otimes^i \Delta x^T] \text{vec}[f_j^{(i)}(x)], \quad (\text{A2})$$

where the notation $[\otimes^j \Delta x^T]$ indicates the Kronecker product between j copies of Δx , e.g., $[\otimes^3 \Delta x^T] = \Delta x^T \otimes \Delta x^T \otimes \Delta x^T \in \mathbb{R}^{1 \times N^3}$. The expansion (A2) can be substituted into (1) to yield

$$\frac{d\Delta x}{dt} = DF(x)\Delta x + \begin{bmatrix} \sum_{i=2}^{\infty} \frac{1}{i!} [\otimes^i \Delta x^T] \text{vec}[f_1^{(i)}(x)] \\ \vdots \\ \sum_{i=2}^{\infty} \frac{1}{i!} [\otimes^i \Delta x^T] \text{vec}[f_N^{(i)}(x)] \end{bmatrix}, \quad (\text{A3})$$

where $DF(x)$ denotes the Jacobian of the vector field evaluated at x .

APPENDIX B: ASYMPTOTIC EXPANSION OF THE JACOBIAN

Computation of the terms of the phase and isostable response curves requires an asymptotic expansion of the Jacobian. This can also be accomplished with a strategy detailed in [21]. To do so, let $DF(x)^T \equiv \frac{\partial F^T}{\partial x} = [\frac{\partial f_1^T}{\partial x} \dots \frac{\partial f_N^T}{\partial x}]$ with all partial derivatives evaluated at x . Using the notation from Appendix A, one can write

$$\begin{aligned} \left. \frac{\partial F^T}{\partial x} \right|_{x+\Delta x} &= DF(x)^T + [a_1 \dots a_N], \\ a_i &= \sum_{j=1}^{\infty} \frac{1}{j!} ([\otimes^j \Delta x^T] \otimes \text{Id}) \text{vec}(f_i^{(j+1)}), \end{aligned} \quad (\text{B1})$$

where a_i is a column vector, Id is an appropriately sized identity matrix, $f_i^{(i+1)}$ is given in Eq. (A1), and all partial derivatives are evaluated at x .

[1] M. Budišić, R. Mohr, and I. Mezić, Applied Koopmanism, *Chaos* **22**, 047510 (2012).

[2] I. Mezić, Spectrum of the Koopman operator, spectral expansions in functional spaces, and state-space geometry, *J. Nonlinear Sci.* **30**, 2091 (2020).

[3] I. Mezić, Analysis of fluid flows via spectral properties of the Koopman operator, *Annu. Rev. Fluid Mech.* **45**, 357 (2013).

[4] P. J. Schmid, Dynamic mode decomposition of numerical and experimental data, *J. Fluid Mech.* **656**, 5 (2010).

[5] C. W. Rowley, I. Mezić, S. Bagheri, P. Schlatter, and D. S. Henningson, Spectral analysis of nonlinear flows, *J. Fluid Mech.* **641**, 115 (2009).

[6] M. O. Williams, I. G. Kevrekidis, and C. W. Rowley, A data-driven approximation of the Koopman operator: Extending dynamic mode decomposition, *J. Nonlinear Sci.* **25**, 1307 (2015).

[7] E. Yeung, S. Kundu, and N. Hodas, Learning deep neural network representations for Koopman operators of nonlinear dynamical systems, in *2019 American Control Conference (IEEE, 2019)*, pp. 4832–4839.

[8] B. Lusch, N. J. Kutz, and S. L. Brunton, Deep learning for universal linear embeddings of nonlinear dynamics, *Nat. Commun.* **9**, 1 (2018).

[9] H. Arbabi and I. Mezić, Ergodic theory, dynamic mode decomposition, and computation of spectral properties of the

- Koopman operator, *SIAM J. Appl. Dyn. Syst.* **16**, 2096 (2017).
- [10] S. L. Brunton, B. W. Brunton, J. L. Proctor, E. Kaiser, and N. J. Kutz, Chaos as an intermittently forced linear system, *Nat. Commun.* **8**, 1 (2017).
- [11] A. Mauroy, I. Mezić, and J. Moehlis, Isostables, isochrons, and Koopman spectrum for the action-angle representation of stable fixed point dynamics, *Physica D* **261**, 19 (2013).
- [12] D. Wilson and J. Moehlis, Isostable reduction of periodic orbits, *Phys. Rev. E* **94**, 052213 (2016).
- [13] D. Wilson and B. Ermentrout, Greater accuracy and broadened applicability of phase reduction using isostable coordinates, *J. Math. Biol.* **76**, 37 (2018).
- [14] S. Shirasaka, W. Kurebayashi, and H. Nakao, Phase-amplitude reduction of transient dynamics far from attractors for limit-cycling systems, *Chaos* **27**, 023119 (2017).
- [15] A. Sootla and A. Mauroy, Geometric properties of isostables and basins of attraction of monotone systems, *IEEE Trans. Autom. Control* **62**, 6183 (2017).
- [16] A. Mauroy and I. Mezić, Global computation of phase-amplitude reduction for limit-cycle dynamics, *Chaos* **28**, 073108 (2018).
- [17] O. Castejón and A. Guillamon, Phase-amplitude dynamics in terms of extended response functions: Invariant curves and arnold tongues, *Commun. Nonlinear Sci. Numer. Simul.* **81**, 105008 (2020).
- [18] B. Monga and J. Moehlis, Optimal phase control of biological oscillators using augmented phase reduction, *Biol. Cybern.* **113**, 161 (2019).
- [19] D. Wilson, Isostable reduction of oscillators with piecewise smooth dynamics and complex Floquet multipliers, *Phys. Rev. E* **99**, 022210 (2019).
- [20] D. Wilson, A data-driven phase and isostable reduced modeling framework for oscillatory dynamical systems, *Chaos* **30**, 013121 (2020).
- [21] D. Wilson, Phase-amplitude reduction far beyond the weakly perturbed paradigm, *Phys. Rev. E* **101**, 022220 (2020).
- [22] B. Monga, D. Wilson, T. Matchen, and J. Moehlis, Phase reduction and phase-based optimal control for biological systems: A tutorial, *Biol. Cybern.* **113**, 11 (2019).
- [23] M. D. Kvalheim and S. Revzen, Existence and uniqueness of global Koopman eigenfunctions for stable fixed points and periodic orbits, [arXiv:1911.11996](https://arxiv.org/abs/1911.11996).
- [24] A. Sootla, A. Mauroy, and D. Ernst, Optimal control formulation of pulse-based control using Koopman operator, *Automatica* **91**, 217 (2018).
- [25] D. Wilson and J. Moehlis, Extending phase reduction to excitable media: Theory and applications, *SIAM Rev.* **57**, 201 (2015).
- [26] A. J. Roberts, Appropriate initial conditions for asymptotic descriptions of the long term evolution of dynamical systems, *J. Aust. Math. Soc. Ser. B, Appl. Math.* **31**, 48 (1989).
- [27] D. Wilson and J. Moehlis, Isostable reduction with applications to time-dependent partial differential equations, *Phys. Rev. E* **94**, 012211 (2016).
- [28] D. Wilson and S. Djouadi, Isostable reduction and boundary feedback control for nonlinear convective flow, in *Proceedings of the 58th IEEE Conference on Decision and Control* (IEEE, 2019).
- [29] A. Winfree, *The Geometry of Biological Time*, 2nd ed. (Springer, New York, 2001).
- [30] J. Guckenheimer, Isochrons and phaseless sets, *J. Math. Biol.* **1**, 259 (1975).
- [31] P. C. Bressloff and J. N. MacLaurin, A variational method for analyzing stochastic limit cycle oscillators, *SIAM J. Appl. Dyn. Syst.* **17**, 2205 (2018).
- [32] K. C. A. Wedgwood, K. K. Lin, R. Thul, and S. Coombes, Phase-amplitude descriptions of neural oscillator models, *J. Math. Neurosci.* **3**, 2 (2013).
- [33] B. Letson and J. E. Rubin, LOR for analysis of periodic dynamics: A one-stop shop approach, *SIAM J. Appl. Dyn. Syst.* **19**, 58 (2020).
- [34] A. Guillamon and G. Hugué, A computational and geometric approach to phase resetting curves and surfaces, *SIAM J. Appl. Dyn. Syst.* **8**, 1005 (2009).
- [35] D. Jordan and P. Smith, *Nonlinear Ordinary Differential Equations: An Introduction for Scientists and Engineers* (Oxford University Press, Oxford, 2007).
- [36] C. D. Meyer, *Matrix Analysis and Applied Linear Algebra*, Vol. 2 (SIAM, Philadelphia, 2000).
- [37] E. Brown, J. Moehlis, and P. Holmes, On the phase reduction and response dynamics of neural oscillator populations, *Neural Comput.* **16**, 673 (2004).
- [38] D. Wilson, An adaptive phase-amplitude reduction framework without $\mathcal{O}(\epsilon)$ constraints on inputs, [arXiv:2011.10410](https://arxiv.org/abs/2011.10410).
- [39] D. Wilson and S. Djouadi, Adaptive isostable reduction of nonlinear time-varying PDEs with large magnitude inputs, *IEEE Control Syst. Lett.* **5**, 187 (2021).
- [40] D. Gonze, S. Bernard, C. Waltermann, A. Kramer, and H. Herzel, Spontaneous synchronization of coupled circadian oscillators, *Biophys. J.* **89**, 120 (2005).
- [41] B. C. Goodwin, Oscillatory behavior in enzymatic control processes, *Adv. Enzyme Regul.* **3**, 425 (1965).
- [42] D. Wilson and B. Ermentrout, Augmented phase reduction of (not so) weakly perturbed coupled oscillators, *SIAM Rev.* **61**, 277 (2019).
- [43] P. Holmes, J. L. Lumley, G. Berkooz, and C. W. Rowley, *Turbulence, Coherent Structures, Dynamical Systems and Symmetry* (Cambridge University Press, New York, 1996).
- [44] K. Taira, S. L. Brunton, S. T. M. Dawson, C. W. Rowley, T. Colonius, B. J. McKeon, O. T. Schmidt, S. Gordeyev, V. Theofilis, and L. S. Ukeiley, Modal analysis of fluid flows: An overview, *AIAA J.* **55**, 4013 (2017).
- [45] J. R. Magnus and H. Neudecker, *Matrix Differential Calculus with Applications in Statistics and Econometrics* (John Wiley & Sons, New York, 2007).